National Research FLAGSHIPS
Water for a Healthy Country

CSIRO

www.csiro.au

Physical properties of soils/sediments of Lower Murray Lakes and modelling of acid fluxes.

Freeman J Cook, Gordon McLachlan, Emily Leyden and Luke Mosley

Report

Prepared for: Department of Environment and Natural Resources' Lower Lakes and Coorong Recovery program.

Government of South Australia

Australian Government

Water for a Healthy Country Flagship Report series ISSN: 1835-095X

Australia is founding its future on science and innovation. Its national science agency, CSIRO, is a powerhouse of ideas, technologies and skills.

CSIRO initiated the National Research Flagships to address Australia's major research challenges and opportunities. They apply large scale, long term, multidisciplinary science and aim for widespread adoption of solutions. The Flagship Collaboration Fund supports the best and brightest researchers to address these complex challenges through partnerships between CSIRO, universities, research agencies and industry.

The Water for a Healthy Country Flagship aims to provide Australia with solutions for water resource management, creating economic gains of $3 billion per annum by 2030, while protecting or restoring our major water ecosystems. The work contained in this report is collaboration between CSIRO and the South Australian Department of Environment and Natural Resources and the South Australian Environmental Protection Agency.

For more information about Water for a Healthy Country Flagship or the National Research Flagship Initiative visit www.csiro.au/org/HealthyCountry.html

Lower Lakes and Coorong Recovery is part of the South Australian Government's $610 million Murray Futures program funded by the Australian Government's $12.9 billion Water for the Future program.

Citation: Cook F.J, McLachlan, G., Leyden, E. and Mosley, L., 2011. Physical Properties of Soils/Sediments of Lower Murray Lakes and Modelling of Acid Fluxes. CSIRO: Water for a Healthy Country National Research Flagship

Lower Lakes and Coorong Recovery is part of the South Australian Government's $610 million Murray Futures program funded by the Australian Government's $12.9 billion Water for the Future program.

Cover Photograph: Taken by Gordon McLachlan CSIRO Land and Water, 2011 of Lake Albert with South Australian EPA boat used for sampling in foreground.

CONTENTS

Acknowledgments ..... **vi**

Executive Summary ..... **vii**

1. Introduction **1**

1.1. Review of Existing Studies 3

1.2. Conceptual Model 4

1.2.1. Initial Lake level reduction 4

1.2.2. Refilling of lake after initial reduction 8

1.2.3. Reduction in lake level following a refilling event 9

1.3. Scope of this Report 10

2. Methods **10**

2.1. Sample Collection 10

2.2. Sites 12

3. Laboratory Methods **12**

3.1. Diffusivity measurements 12

3.1.1. Experimental apparatus 12

3.1.2. Experimental procedure 14

3.1.3. Theory and analysis 16

3.2. Moisture characteristics 17

3.3. Coefficient of Linear Extensibility (COLE) 19

3.4. Particle Size 19

4. Results **20**

4.1. Diffusivity experiments 20

4.1.1. Desorptivity 20

4.1.2. Diffusivity 23

4.1.3. Estimating Saturated Hydraulic Conductivity (K_s) from the Drying Data 25

4.2. Moisture Characteristics 27

4.3. Coefficient of Linear Extensibility (COLE) 28

4.4. Particle Size Analysis 32

4.5. Numerical Modelling 34

5. Modelling **34**

5.1. Comparison of Simulations with Piezometric Head Data 34

5.1.1. Comparison with Point data Using Under Atmospheric Boundary Conditions 34

5.1.2. Comparison with Transects During Drying Phase 37

5.2. Water transport from the Lake 38

5.3. Water and Oxygen Penetration into Peds 40

5.4. Rewetting of Peds and Solute Transport out of Peds 43

6. Discussion **47**

6.1. Measurements 47

6.2. Modelling 49

7. Summary and conclusions **52**

8. RecoMmendations for further research **52**

9. References **54**

10. Appendix 1 ..... **57**

LIST OF FIGURES

Figure 1. Historical water levels at Lock 1 and Lake Alexandrina. Data supplied by Luke Mosley SA EPA. 1

Figure 2. Schematic of the initial reduction of the lake water level a) initial water level and lake radius of R_0 and b) at a level Δh below the initial level. 5

Figure 3. Schematic of formation of acid salts at the sediment surface and subsequent acid flux due to washing of acid products from near lake zone. The water table height will fluctuate in the sediments which can also result in exfiltration causing acid salts to be washed from the surface. 6

Figure 4. Flux of acid to the lake via groundwater a) fluxes in the profile b) exfiltration from a seepage face to the lake. 7

Figure 5. Schematic of cracking of clay sediments, with ped radius and crack depth indicated. The cracking pattern in reality is likely to be more hexagonally shaped than cylindrical but hexagonal columns can be approximated as a cylinder (Scotter et al. 1978)... 8

Figure 6. Cracked clays at Dunn's lagoon showing acidic water (Inset: pH 2.52) in crack prior to rewetting (Source: EPA) 9

Figure 7. Photo showing sample collection at Campbell Park site. 11

Figure 8. Photograph of sampler, showing auger tube, a sample in liner, sample catcher (yellow plastic), plastic liner for sample and cutting shoe. Image from Dormer Engineering. 11

Figure 9. Photographs showing a) samples with duct taped ends and b) tube used for storage and transport of samples. 12

Figure 10. Schematic of experimental apparatus for measuring diffusivity of soil core samples. A thermistor measures the temperature in the box and a light bulb (heat source) is switched on and off to maintain the temperature at approximately 25°C. 13

Figure 11. Photo of core in diffusivity apparatus prior to start of test showing the balance, light bulb, mesh floor and data logger. This core had both ends enclosed and to check water loss through the heat shrink plastic. 13

Figure 12. Temperature versus time for box. The initial period before the switching can be seen is due to the box temperature being > 25°C. 14

Figure 13. Mass loss from sealed core over a 6 day period. 15

Figure 14. Cutting up sequence for core upon removal from the diffusivity apparatus: a) prior to sectioning; b) first few samples sectioned, c) about half of core sectioned and d) cores after oven drying. 16

Figure 15. Pressure plate showing sub-samples and heat shrink liner. Some shrinkage can be seen with some of the samples. 18

Figure 16. Mass loss from core BL8 in the initial stages of drying. The arrow showing the break in the slope is where it is assumed stage one drying of the core started. The regression shown is used to determine the steady-state and maximum evaporation rate used in the HYDRUS 1D inverse modelling. 20

Figure 17. Evaporation (m) versus square root of time ($s^{1/2}$) for core PS5 during the second stage of drying. 22

Figure 18. Water content (θ) versus Boltzman transform ($xt^{-1/2}$) for Boggy Creek cores. The data enclosed in the box were removed from the data set as being unreliable when fitting eqn (7). 23

Figure 19. Fit of eqn (7) to experimental data from Boggy Creek diffusivity experiments, with exclusion of data indicated in figure 18..... 24

Figure 20. The diffusivity (*D*) as a function of reduced water content (*Se*) for the Boggy Creek site calculated with eqn (8) and the parameter values in Table 4. 25

Figure 21. Mean COLE at average depth of sample for all sites. The error bars are the standard deviation of the 3 replicates. 29

Figure 22. Campbell Park site during piezometer installation showing absence of cracking (from Earth Systems 2008). 29

Figure 23. Point Sturt site during piezometer installation showing absence of cracking (from Earth Systems 2008). 30

Figure 24. Boggy Lake under drying illustrating cracking of the surface. 30

Figure 25. Photograph showing cracking of sediments and infilling at Boggy Creek site. (Photograph by Dr R. W. Fitzpatrick). 31

Figure 26. Saturated water content (θ_s) range and mean for the four sites derived from the particle size data using the method of Saxton et al. (1986). 33

Figure 27. Saturated hydraulic conductivity (K_s) range and mean for the four sites derived from the particle size data using the method of Saxton et al. (1986). 33

Figure 28. Comparison of HYDRUS2D simulation of water table (z_{WT}) behaviour at the Campbell Park site. The points are the measurement points (Earth Systems 2010) in a transect at this site (see Earth Systems (2010) and Cook (2011) for more details). 35

Figure 29. Comparison of simulations with average, minimum and maximum soil properties for the Campbell Park site for the depth of water table below the surface (z_{WT}) with data from point 1 of the piezometer transect. 35

Figure 30. Comparison of HYDRUS2D simulation of water table (z_{WT}) behaviour at the Point Sturt site. The points are the measurement points (Earth Systems 2010) in a transect at this site (see Earth Systems (2010) and Cook (2011) for more details). 36

Figure 31. Comparison of simulations with average, minimum and maximum soil properties for the Point Sturt site for the depth of water table below the surface (z_{WT}) with data from point 1 of the piezometer transect. 36

Figure 32. Comparison of the transect simulations of water table height (z_{WT}) simulated for points 2 and 3 with measured piezometric heads for Campbell Park site. 37

Figure 33. Comparison of the transect simulations of water table height (z_{WT}) simulated for points 2 and 3 with measured piezometric heads for Point Sturt site 38

Figure 34. Flowing particle tracks (pink lines) at; a) points 2 and 3 in transect for Point Sturt and b) point 1 in transect at Campbell Park. 38

Figure 35. Particle tracks (pink lines) for flowing particles due to water intake at the lake sediment boundary for the Point Sturt sediment with a constant evaporation rate of 4 mm day^{-1}. The horizontal grid cell mesh size is 1.067 m. The particles were initial sited on the outer edge of the domain (left hand edge). The coloured bards at the top beyond 5 m are due to the low potential values caused by drying of the sediments. 39

Figure 36. Concentration of oxygen (C) in relation to the maximum concentration (C_0) with depth, at the centre (r = 0) and ped surface (r = R), where R = 0.05 m, the crack length is 0.25 m and the water table is maintained at 0.5 m. 42

Figure 37. Research strategy for improvement of knowledge. 43

Figure 38. HYDRUS2D simulations of solute transport in peds with radius of 0.05 m, and crack depth on right hand side of 0.25 m and water table depth during drying of 0.5 m for

Boggy Creek sediment; a) distribution of oxygen after 1000 of drying, b) distribution of solute after 100 days of rewetting with water only in crack and c) distribution of solute after 100 days of rewetting with water in crack and on the surface. The absolute solute scale is not shown as the scales are different for panel a compared to panels b and c. The scale represents the relative concentration. 44

Figure 39. HYDRUS2D simulations of solute transport in peds with radius of 0.15 m, and crack depth on right hand side of 0.50 m and water table depth during drying of 0 m for Boggy Creek sediment; a) distribution of oxygen after 1000 of drying, b) distribution of solute after 100 days of rewetting with water only in crack and c) distribution of solute after 100 days of rewetting with water in crack and on the surface. A relative scale is shown. 45

Figure 40. Percentage mass lost with time for peds with; a) radius of 0.05 m and different crack depths and drying water table depths, and b) crack depth of 0.5 m and drying water table depth of 0.5 m and different ped radii. The sediment properties were those from Boggy Creek. 46

Figure 41. Percentage of solute mass lost with time for sediments inundated with water on the sediment surface following a long period of drying for all four sites. 47

Figure 42. Cracking clays at Boggy Lake rewetted with pH 3 water (Source: EPA)..... 49

Figure 43. Acidification events recorded in the Lower Lakes from 2007-2010 (Source: EPA). 50

Figure 44. Time course for pH in a) Boggy Lake and b) Boggy Creek following refilling of the lakes. The dashed lines on the Boggy Lake graph indicate when aerial limestone additions to the water body occurred (Source: EPA). 51

LIST OF TABLES

Table 1. Position of the sampling sites. 12

Table 2. Particle size range for soil texture using the Australian standard and USDA standard (Cook and Cresswell 2008). 20

Table 3. Desorptivity estimates from drying of cores in diffusivity apparatus. 22

Table 4. Parameters derived by fitting eqn (7) to the experimental data for Boggy Creek. The desorptivity estimated from eqn (9) (D_e^*) is also shown. 24

Table 5. Estimated van Genuchten parameters and saturated hydraulic conductivity from inverse modelling of diffusivity experiments. The mean values are shown for each site with the standard deviation in brackets. 26

Table 6. van Genuchten's parameters fitted using RETC to the mean, maximum and minimum data sets at each depth increment. 27

Table 7. Estimates of capillary length scale (λ_c) using eqn (13) and from field measurements (Cook 2011). 28

Table 8. Particle size of samples from sediments at Campbell Park (CP), Point Sturt (PS), Boggy Creek (BC) and Boggy Lake (BL). The depth increment and site are in column 1 and texture in column 7. 32

Table 9. The estimated distance that the boundary condition imposed by the lake influences water flow from the lakes to the sediments (X_p) and the pressure head (X_h). These distances were calculated after 4 mm day^{-1} of evaporation for 1000 days. 40

Table 10. Oxygen penetration depth (z_{O2}) in peds in relation to crack length (z_c), ped radius (r) and water table depth (z_{WT}) at the centre of the ped (r = 0) and at the radius of the column (r = R). 41

Table 11. The proportion of solute mass lost from the peds upon rewetting after 1000 days of water in the crack to the crack depth but not on the sediment surface (M_0) and when water is also on the sediment surface (M_s). 44

Table 12. Comparison of air-entry values from (monitoring data, ψ_{ie}) and laboratory data (ψ_{il}) and capillary length scale (λ) for Point Sturt and Campbell Park sites. 48

Table 13. Moisture characteristic and bulk density (ρ_b) for Boggy Creek Site. 57

Table 14. Moisture characteristic and bulk density (ρ_b) for Point Sturt Site. 58

Table 15. Moisture characteristic and bulk density (ρ_b) for Campbell Park Site. 59

Table 16. Moisture characteristic and bulk density (ρ_b) for Boggy Lake Site. 60

ACKNOWLEDGMENTS

This work was jointly funded by the South Australian Department of Environment and Natural Resources (DENR) and CSIRO Water for a Healthy Country Flagship. The author would like to thank Dr Liz Barnett (DENR), Dr Paul Shand (CSIRO), Mr David Ellis (CSIRO) and Mr Peter Williams (CSIRO) for their assistance with obtaining the funding. The sediment sampling assistance of Benjamin Zammit and Darren Green (EPA) is also greatly appreciated.

EXECUTIVE SUMMARY

This is the second report on the likely acid fluxes from the pyrite-containing (sufidic soil) sediments exposed on the margins of the Lower Lakes of South Australia following large water level declines. This report concentrates on the fluxes that will be generated upon rewetting of the sediments and diffusion of acidity back into the surrounding water. In order to be able to model these processes the physical properties of the sediments are required to be measured or estimated.

Sediment samples were taken from the Lower Lakes at two locations each in Lake Albert and Lake Alexandrina. These samples represented sandy and clayey sediments from each of the lakes. Due to the refilling of the lakes, sediment cores were collected with a small diameter tube auger. The physical properties of these sediments were then measured using standard soil physical methods except for the soil water diffusivity. The soil water diffusivity was measured using a specially built apparatus which monitored the mass of water lost from the sediments during drying from one face of the core samples. This data was then used along with the HYDRUS1D modelling program to estimate the hydraulic conductivity using inverse modelling. These values along with the moisture characteristics and bulk densities were used with the HYDRUS2D/3D model to simulate oxygen, water and solute movement into the sediments.

The coefficient of linear extensibility (COLE) was measured on the samples and showed that the clayey sediments had considerable ability to change their density and porosity upon drying and cracking. This cracking had been observed during the drying of the lakes from 2006 until 2010. Modelling of oxygen penetration into the peds formed by this cracking was undertaken. The results indicated that oxygen penetration would be controlled by both the crack and water table depth for peds with diameters less than 20 cm, but for peds as large as 30 cm in diameter or greater the oxygen penetration was limited in the centre of the ped.

At two sites, Campbell Park and Point Sturt, piezometric level monitoring data enabled comparisons to be made between the simulated and measured behaviour. The simulations were similar during the drying phase of the sediments but did not show the same response to rainfall as the monitoring. This is possibly due to the hysteresis in the moisture characteristic (the relationship between water content and matric potential is different depending on wetting or drying of the sediments) which was not accounted for in the simulations.

Simulations using flowing particles indicated that the influence of the water from the lakes on the drying of the sediments was much less than had been estimated in the first report (Cook, 2011). This was due to overestimation of the macroscopic capillary length scale in the earlier report. Water from the lake was found to influence the head to less than 10 m from the water's edge for all the sediments.

The simulations confirmed the earlier findings of Cook (2011) that the water flow in the exposed sediments would be mainly vertical and driven by to evaporation and rainfall. They also confirmed the suggestions by Cook (2011) and Hipsey et al. (2010) that lateral groundwater flow was an unlikely mechanism for significant acid transport to the lakes.

The diffusion of a passive solute from the peds (cracked clayey sediments) and non-cracked sediments to the surrounding water was simulated using HYDRUS2D/3D. This showed that the cracking of the sediments would result in enhanced transport of acidity to the surrounding water by up to 30%. The rate of release is also different for the peds compared to flat sediments, with continued release of solutes to the surrounding water for the peds. These simulations give similar results to the mesocosm experiments of Hicks et al. (2009) and field observations which adds credence to these simulations.

The simulations indicated that a rapid release of acidity would occur upon rewetting of the sediments with almost no further release from the flat sediments and a slow continued release from the peds. This means that the most dangerous period for acidification of the lakes is immediately after a rapid refilling when acidity will be transported to the water above the sediments especially from the cracked clayey sediments. Following this period only the clayey sediments are predicted to continue to release acidity to the surrounding water. These findings are generally consistent with field observations. The simulated release is likely to overestimate this rate of release as collapsing of the peds and filling of the cracks with sediment will slow the release. However, this process may also enhance the initial release of acid.

These results suggest that if the lakes have not turned acidic upon refilling they are unlikely to do so in the future under a relatively stable water level outlook. However, monitoring of areas of where clayey sediments occur would be judicious given the slow release of acid suggested by these simulations.

Further research on monitoring of especially the clayey areas and installing some control sites is suggested. Further column studies and modelling using coupled PHREEQC and HYDRUS2D/3D to better understand the sulfate reduction dynamics and risks posed by future drying events is suggested.

1. INTRODUCTION

The Lower Lakes (Lakes Alexandrina and Albert) are located near the mouth of the Murray River in South Australia approximately 75 km south of Adelaide. The drought in the Murray Darling Basin has resulted in lower flows of water through the Murray River to Lake Alexandrina and Lake Albert. The Lakes were full in 2006 but by 2008 water levels had dropped to sea level (Figure 1). The lower water level in the Lower Lakes have exposed sediments with pyrite concentrations that can generate a potential net acidity of > 250 mol H^+ $tonne^{-1}$ in some of the sediments, with the majority of the sediments having acidity generating capacity of less than this, but some sediments especially in Lake Albert having high > 500 mol H^+ $tonne^{-1}$ capacity (Fitzpatrick et al. 2010). The lakes are alkaline and have considerable buffering capacity but the acidity potential is much greater and even if a small percentage of this acidity was transported to the lakes it is possible that the lakes could become acidic (Hipsey and Salmon 2008). However, for the acid sulfate hazard in the sediments to become a risk to the lake, the acidity must be transported from the sediments to the lake waters.

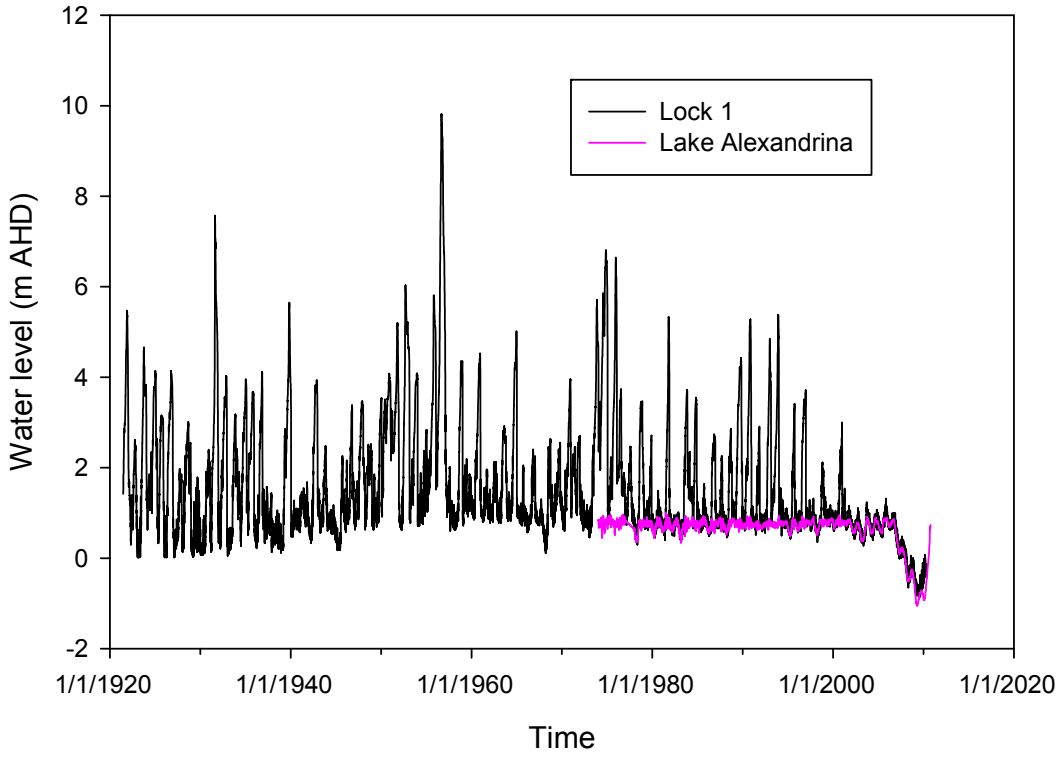

Figure 1. Historical water levels at Lock 1 and Lake Alexandrina. Data supplied by Luke Mosley SA EPA.

Modelling has been done of the acid generation and flux (Hipsey and Salmon 2008; Hipsey et al. 2010) and lake processes. This is based on laboratory estimates of the oxidation rate of the pyrite (Earth Systems 2010) and modelled groundwater flux as the major mechanism for acid flux to the lakes. These oxidation rate studies gave the potential oxidation rate as they were conducted with atmospheric oxygen concentrations. Atmospheric oxygen conditions are unlikely to occur throughout the sediments due to consumption of oxygen by organic reactions and by the pyrite oxidation itself (Cook et al., 2004). Rigby et al. (2004) and Cook et al. (2004) showed that oxidation of organic matter competes for oxygen with pyrite oxidation and can reduce the amount of oxygen available for pyrite oxidation. The planting of vegetation and the natural revegetation will result in competition for the oxygen by plant roots (Cook and Knight 2003). However, some plants have aerenchyma (canals that

can transport air to roots), especially those that can survive in high iron and sulfate environments such as *Phragmites australis* (Armstrong and Armstrong 1988). These plants can release oxygen to the soil around the roots and may cause an increase in the pyrite oxidation in these oxygenated sediments. Observations of iron formation in the vicinity of such roots suggest that these plants are likely to exacerbate acid generation. Modelling of the oxygen transport into the sediments can be performed using such models as HYDRUS-2D/3D (Šimůnek and Šejna 2007) and can give a better estimate of the likely oxidation rates and in relation to depth and water content of the sediment profile.

The gradient for flow to the lakes from the surrounding sediments is not large and evaporation in the sediments near to the water's edge is likely to cause a gradient from the lake to the sediments during the falling stage of the lake level, especially in these shallow flat-bottomed lakes during the warmer months when evaporation is highest. When lake levels rise again the gradient is likely to be predominantly away from the lake. This mechanism has been investigated by Cook (2011) in a recently published report and was shown to be unlikely to generate acid fluxes of any significance.

Cook (2011) developed a conceptual model of the acid flux to the lakes and considered that the flux would be generated from four major mechanisms:

- washing of acid products from the surface of the oxidised sediments during seiching and rainfall,
- flow of acidic groundwater to the lake,
- exfiltration (loss of water from the soil due to pressure) of acid pore water during rainfall events or upon rewetting of near shore sediments,
- diffusion and/or mixing of the acidity in the sediments into the lake waters during seiching events or upon flooding following lake level rise.

Cook (2011) went on to analyse existing hydrological and chemistry data sourced from Earth Systems (2010) and EPA (2011). From this analysis he suggested that exfiltration and washing off of acid salts from the exposed sediment surface during runoff events were the most likely source of acid flux to the Lower Lakes. He also stated that there was a need for measurements of the physical properties of the sediments to be able to model the processes and to have better data to use in these models.

The measurements and modelling will help to address the objectives of the South Australian Government to:

- Develop an understanding of the acidity generation, neutralisation and groundwater transport processes within the lake sediments of the Lower Lakes.
- Quantify acidity flux rates to proximal water bodies during wetting events, by assessing the hydrogeology and hydrogeochemistry of lake sediments via a combination of laboratory and field test work programs.
- Provide recommendations for future management of the Lower Lakes.

Here we will present measurements of the relevant physical properties of the sediments which will allow a better understanding the behaviour of sediments during wetting and drying and transport properties. We will present a conceptual model for transport of acidity from the sediments to the lakes due to diffusion of the acid solutes out of the sediments, particularly for the clay-dominated sediments where shrinkage and cracking upon drying will increase the surface area. Modelling will be used to provide insight into the processes for acid flux identified in the first report and the diffusion processes investigated here.

1.1. Review of Existing Studies

The mapping studies by Fitzpatrick et al. (2008, 2010) have described the potential acidity generation and extent of acidity that could be produced if all the pyrite in the sediments was oxidised. However, the rate of generation and transport of acidity to the lake waters was not addressed in this study. A subsequent study by Simpson et al. (2009, 2010) in which samples of the acid sulfate sediments were dried, and then rewetted by shaking in water sourced from the Murray River, and artificial rainwater, gave estimates of the likely maximum acid released into the water. However, the treatment of these samples would have exaggerated the transport from the sediment to the water. This study also showed that if the ratio of Murray River water (alkaline) to suspended acidic sediments was less than 100:1 the solution pH will drop to 6.5. Also the amount of precipitation of metals (Al and Fe) is close to 100% at this dilution, which will maximise the acid release. They also suggested "Flow pathways and interactions with sub-surface waters in the river, wetlands, ground waters (that usually have high alkalinity) and lakes are poorly defined, but may have a significant effect on the degree to which soil waters are neutralised. Detailed studies are recommended for those wetlands likely to be at risk from acidification by ASS".

To estimate the likely risk to the lakes, modelling of the acid flux to the lakes, along with subsequent mixing and reaction within the lakes was performed by Hipsey and Salmon (2008). Their results suggested that the Lakes could become acid, if water levels fell below -1.11 to -2 m. Their interim report was criticised by Webster et al. (2008), in particular the oxidation rates and acid flux transport mechanisms that were assumed. This lead to a revision and the published report by Hipsey and Salmon (2008) included suggestions from Webster et al. (2008). However despite the uncertainties noted in the earlier Hipsey and Salmon report, their modelling successfully predicted Loveday Bay and Currency Creek acidification in winter 2009 assuming average oxidation rate scenarios (DENR 2010).

This review led to further studies to better quantify the oxidation rate of the sediments, effects of flooding with fresh and saltwater on acid release and sulfide reduction, water table heights, water content profiles and groundwater quality, and further modelling.

Knowing the oxidation rate of the sediments is important to be able to estimate the rate of acidity generation as well as the profile of acidity as a function of depth in the sediments. Earth Systems (2010) has made estimates of the oxidation rate as functions of water content and obtained a maximum rate similar to Rigby et al. (2004) for stirred suspended sediment. They did not assess the likely *in situ* rate when oxygen transport and consumption by organic matter occurs. Rigby et al. (2004) found even in their well-stirred experiments, which maximise possible oxidation, that most of the oxygen was consumed by organic reactions. Thus, the use of the oxidation rate from Earth Systems (2010) for the sediments is likely to overestimate oxidation and acid generation.

Experiments using mesocosms in which oxidised sediments were mixed with either river water or saltwater were carried out by Hicks et al. (2009), showed that much less acidity is transferred to the water column when river water was used than would be predicted by Simpson et al. (2009). They also showed increased acid release when saltwater was used, which suggested that flooding the sediments with saltwater could exacerbate the acid transfer to the lake waters. The experiments of Hicks et al. (2009) do not have the degree of wave action that will occur in the lakes or the alternate wetting and drying caused by seiching and are likely to underestimate the flux upon rewetting. These experimental results (Hicks et

al. 2009) provide estimates of the rate of reduction of sulfate compared to diffusive flux, which is important in determining the time course of acid release upon rewetting.

Sulfate reduction studies (Sullivan et al. 2009) have shown that lack of carbon is likely to limit the sulfate reduction processes when the sediments are rewetted by lake level rise. Further *in situ* studies are required to determine the oxidation rate and penetration depth of drying fronts into the sediments, especially the clays. Hicks (unpublished report) has recently been able to model the reaction rates within the mesocosm experiments and this modelling will also add to the understanding of sulfate reduction processes.

The water table transects and water content profiles were monitored by Earth Systems (2010) and EPA (2011) for three transects and provide a very valuable data set, which were used by Cook (2011) to determine hydraulic gradients and likely acid fluxes. He showed that the flux via the groundwater was unlikely to have significantly contributed to acid flux to the lakes due to the small gradients. He subsequently showed that the most likely cause of acid flux was due to exfiltration and runoff. However, no modelling of these processes was undertaken to determine the likely mass of acidity transported, just the maximum likely to be transported.

On the basis of the further information on oxidation rates and groundwater transects Hipsey et al. (2010) subsequently modified their original model and provided revised estimates of acid fluxes to the lakes. This modelling still does not consider some of the transport mechanisms that were discussed by Cook (2011) and briefly presented in section 1.2 below and may have overestimated the acid fluxes to the lakes. An expansion of the conceptual model for diffusive flux will be presented here.

1.2. Conceptual Model

The conceptual model considers three scenarios *viz* initial lowering of the lake levels, refilling, and subsequent lowering of the lakes.

1.2.1. Initial Lake level reduction

The initial lake level reduction will expose sediments and these will become unsaturated to some depth away from the lake (Figure 2). These unsaturated sediments can then generate acidity by oxidation of the pyrite.

The sediments will remain saturated to some distance from the lake water edge, which can be approximated as $\Delta R_\lambda = \lambda / \tan\theta$, where λ is the macroscopic capillary length scale of the sediments (White and Sully 1987), and θ is the angle of the soil surface away from horizontal. This is only approximate, as evaporation will reduce this distance. It can be calculated more precisely if the evaporation rate and soil physical properties of the sediment are known. At distances greater that ΔR_λ the sediments will get progressively more unsaturated as the soil surface rises (depth to water table increases) and pyrite oxidation will increase with this increasing distance from the shoreline. Beyond a certain distance, the evaporation rate will decrease as the transport of water to the soil surface limits the evaporation. This will then decrease the rate of increase in the depth of the drying front and limit the amount of sediment oxidised. This decrease in the drying depth will continue until some point where the upward flux of water due to evaporation becomes negligible.

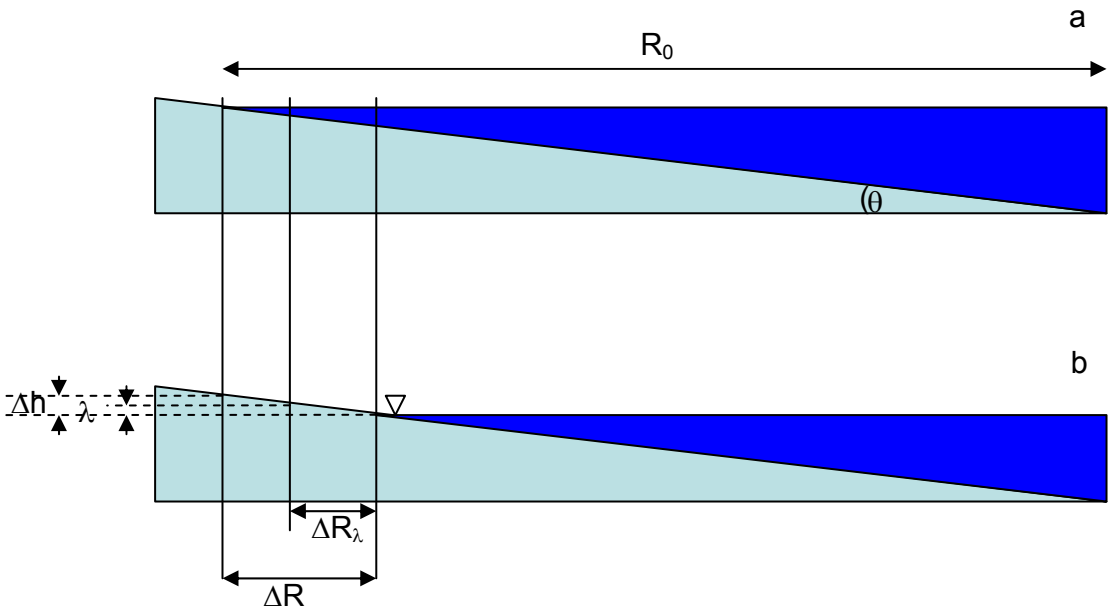

Figure 2. Schematic of the initial reduction of the lake water level a) initial water level and lake radius of R_0 and b) at a level Δh below the initial level.

Acid transport

The mechanisms for acid entering the lake waters are:

- washing of acid products from the surface of the oxidised sediments during seiching and rainfall,
- flow of acidic groundwater to the lake,
- exfiltration of acid pore water during rainfall events or upon rewetting of near shore sediments
- diffusion and/or mixing of the acidity in the sediments into the lake waters during seiching events or upon flooding following lake level rise.

In the near shore region beyond ΔR_λ, evaporation is likely to concentrate acidic salts on or near the soil surface. The amount of water required to saturate the sediments during a rainfall event or seiching will be small and the acidic salts can be washed into lake waters (figure 3). This mechanism is discussed in more detail in Cook (2011).

The amount of acidity generated in this region may be small and regular washing may also reduce the amount available in each event. This region is denoted by $\Delta R - \Delta R_\lambda$ in figure 2. As the water table depth increases the water content at the surface will decrease, and the upward flux will be limited by the hydraulic conductivity of the sediments. The distance to where the upward flux becomes negligible, will be dependent on physical properties of the sediment (macroscopic capillary length scale) and evaporation rate. The acidic salts will also be washed back down the soil profile in rainfall events which do not cause runoff. The amount of acidity in any runoff will depend on the exchange processes between the soil and runoff water. Tong et al. (2010) has developed a model for estimating such processes.

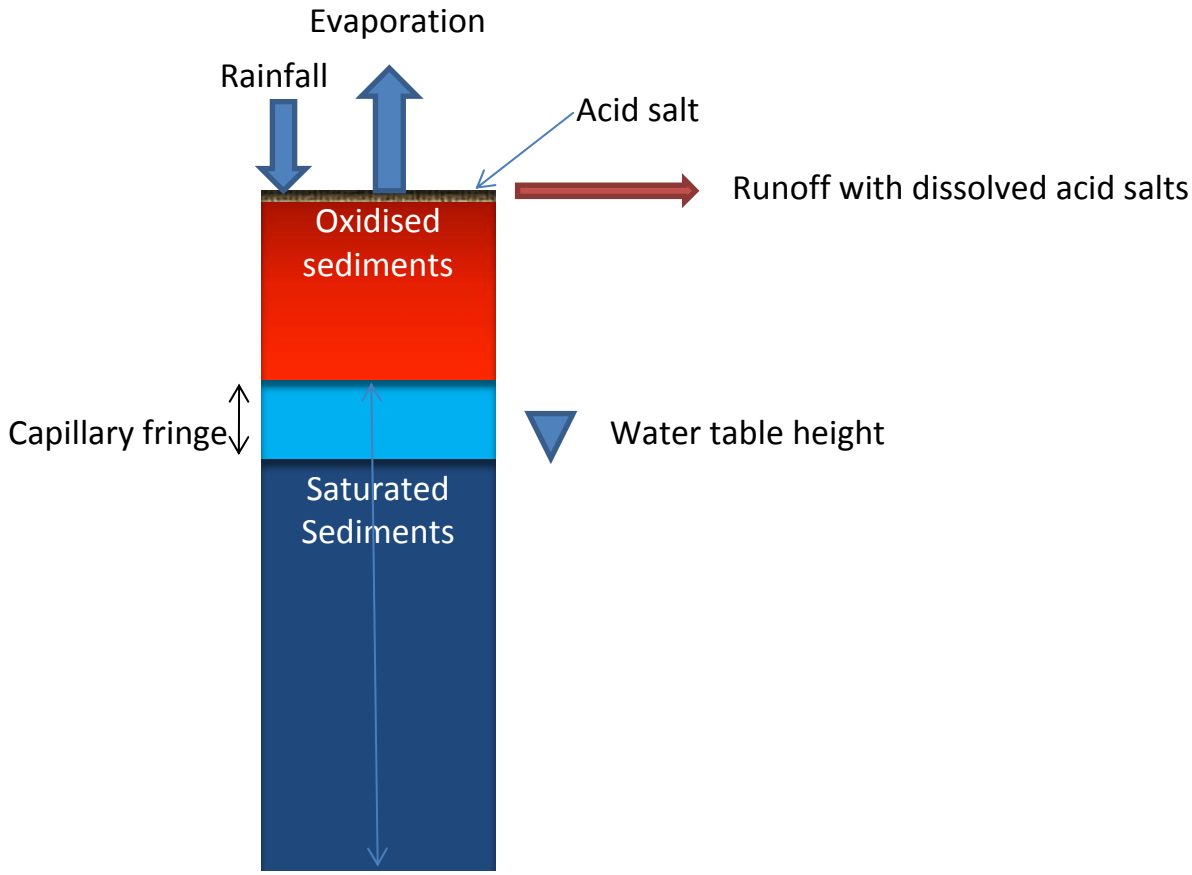

Figure 3. Schematic of formation of acid salts at the sediment surface and subsequent acid flux due to washing of acid products from near lake zone. The water table height will fluctuate in the sediments which can also result in exfiltration causing acid salts to be washed from the surface.

The potential for increased groundwater flux will occur during reduction in the lake water, which potentially induces a flux of water to the lake as the hydraulic gradient steepens. This process will not result in acid flux until the acidic products from the oxidation are washed down to the water table. Groundwater flux to the lake will also occur following rain, when the water table on the land surrounding the lake rises (due to infiltration of rainfall) and results in a gradient towards the lake. There are a number of parts to this process. Firstly the acidic products need to be washed down to the groundwater through the unsaturated soil zone and/or the water table rises into the oxidised zone and solubilises retained acidity. Depending on the amount of drainage, some reduction in concentration will be possible if the flux through the saturated zone near the water table is slower than the rate of sulfate reduction, or acidic groundwater passes through unoxidised sediments with carbonate content (Figure 4a).

Secondly the acidic groundwater needs to be transported into the lake. The groundwater flux will also be reduced by evaporation in the near shore region, lowering the water table in this region and resulting in water flux from the lakes to the sediment and/or reducing the overall hydraulic gradient. This has been observed in data collected by Earth Systems (2010) and EPA (2011). This will mean that the groundwater flux is only likely to occur when rainfall has caused a significant water table gradient towards the lake. However, the travel time for the flux of acidity from drier more acidic regions upslope may be considerable, and estimation of the travel distances and times will be helpful in understanding the potential future acidic fluxes.

However, the groundwater pressure from upslope can also cause the water table near the lake to rise above the surface of the sediments and for exfiltration to occur. This exfiltration can cause the washing off of acidic salts (Figure 3) and water rising up through the oxidised zone is likely to contain acidity, and this mechanism will constitute a pathway for acid flux to the lakes (figure 4b). Exfiltration in the near shore area is also possible due to lake level rise during seiching events or lake refilling as the water pressure from the lake can cause water to exfiltrate from the sediments.

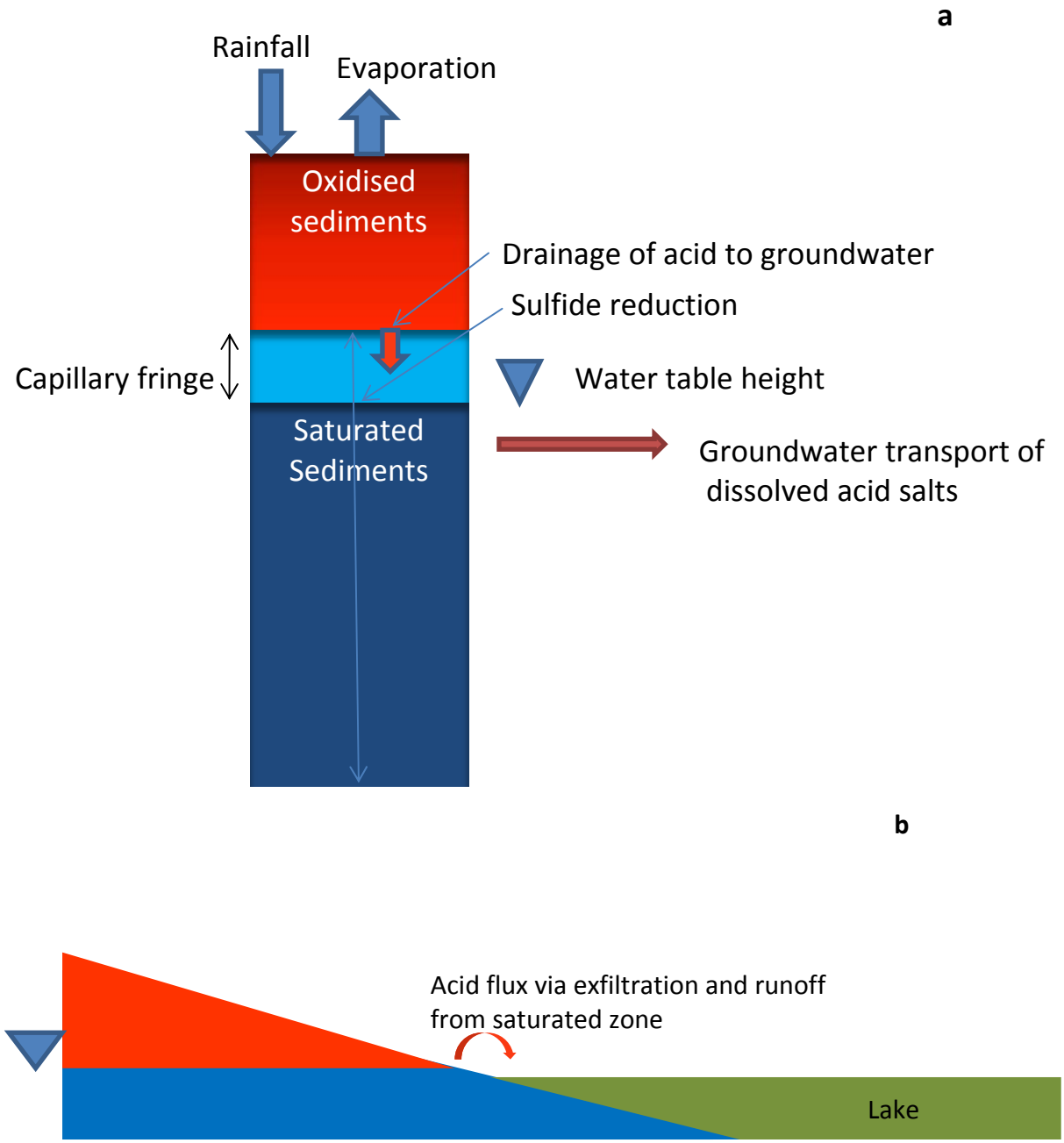

Figure 4. Flux of acid to the lake via groundwater a) fluxes in the profile b) exfiltration from a seepage face to the lake.

The third mechanism for acid flux into the lake is during seiching events, when the acid can move from the sediments to the lake water via dissolution of acidic salts on the surface of the sediment, diffusion from the sediments, and/or convection induced by wave action. Negligible acid flux for diffusion is likely as the seiching events will be of a short duration and

diffusion will need a long time for it to result in any acid transport to the lake water. These events will occur in the near shore region where flow of water from the lake is likely to have minimised acid generation.

The generation of acidity, which will be available for release upon refilling of the lakes will be generated following this draining phase of the lakes. This acid generation will be enhanced in the clayey sediments by the formation of cracks. This will expose a greater surface area of the soil to the atmosphere, and increase water loss (Adams and Hanks 1964) and oxygen penetration into and pyrite oxidation in the sediments.

1.2.2. Refilling of lake after initial reduction

The refilling of the lake after the initial drop in lake level to some minimal value will result in a rising water table level in the near shore region. This is likely to suppress the groundwater flux to the lake and result in alkaline lake water flowing into acidic sediments. However, this may also cause a flux of acid water to be pushed up out of the soil (exfiltration) in the region ΔR_{λ} away from the new lake level (Figure 4b). It was observed that along this transect in depressions pooled water occurred with a measured pH of 3-4. Sulfate reduction is also likely to be initiated in this region due to the saturated anoxic conditions. As the water level in the lake rises, the region where acidic products can be washed off by rainfall will extend into areas of increased acidity. The inundation of previously dry, acidic sediments will lead to an increase in the flux of acidity from diffusive and convective processes.

The diffusion process is likely to be very slow but dissolution and advection due to wave action and/or resuspension of the sediments will be a much faster process and likely to be closer to the results of Simpson et al. (2009, 2010) for the shaken oxidised sediments. The higher surface area due to cracks in the clay sediments will increase the surface area for diffusion and the flushing of acidity by convection (Figure 5).

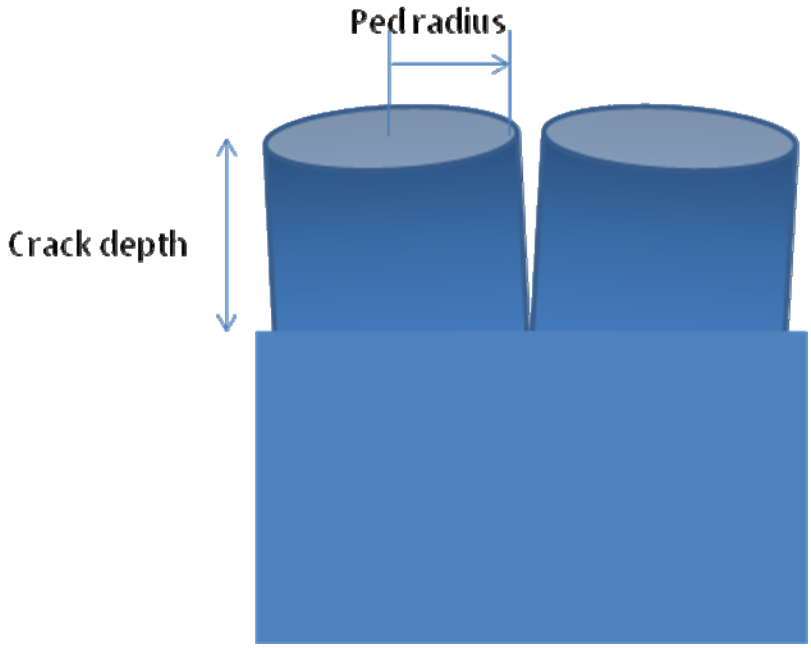

Figure 5. Schematic of cracking of clay sediments, with ped radius and crack depth indicated. The cracking pattern in reality is likely to be more hexagonally shaped than cylindrical but hexagonal columns can be approximated as a cylinder (Scotter et al. 1978)

For clays this process may be important especially after lake refilling. The rewetting of these clays will cause water to be absorbed and advected into the sediment columns from both the

surface of the columns as well as the sides. Depending on the rate of refilling, the cracks may have acidic water in them for a considerable time before the water also starts to infiltrate from the surface of the peds (see Figure 6). This could result in transport of solutes up the sides and towards the surface of the sediment columns compared to when overtopping of the whole column occurs when the advective flux may result in solutes being carried away from the surface of the columns.

Figure 6. Cracked clays at Dunn's lagoon showing acidic water (Inset: pH 2.52) in crack prior to rewetting (Source: EPA)

The clays are also highly sodic and dispersive, which means that the cracks may fill through collapse of the peds upon lake refilling, so transport from the sides of the columns may be a relatively short lived process. This dispersion and collapse of the peds is however, likely to expose the oxidised sediment to interaction with the lake water and enhance the transport of acidity to the lake initiallyThese processes can be modelled as a series of scenarios and the relative amount of solute (acid) flux can be estimated for each of these scenarios. However, observations so far show the cracks and ped structure have remained.

1.2.3. Reduction in lake level following a refilling event

Sediments exposed prior to refilling will have oxidised and formed sulfates. Upon refilling these sediments will get inundated and sulfate reduction is likely to occur, resulting in generally mono-sulfides being produced. Monosulfidic-black-oozes (Bush et al. 2004) can also form if enough organic matter is present some has been found Kennedy Bay and Ewe Island Barrage (Dr A. K. Baker pers. comm. 2011).

Subsequent reduction in the lake level will expose these monosulfides which can quickly oxidise to produce a source of acidity near to the lake water level. This acidity can be transported to the lake waters via seiching, wave action and wash off by rain in the near shore region. This could result in pulses of acidity into the lake waters when seiching or rain occurs.

1.3. Scope of this Report

This report will give detailed measurements of the physical properties of the sediments in particular: the moisture characteristics, the desorptivity, the bulk density, coefficient of linear shrinkage and the soil water diffusivity. From these data the hydraulic conductivity as a function of water content will also be derived. These data will be used along with modelling to estimate fluxes of oxygen, water and solutes in the sediments and estimate the range in the flux of acidity to the lakes for various scenarios. The HYDRUS suite of models will be used for the modelling and also used via inverse modelling to get the hydraulic conductivity functions of the sediments.

This report will complement and extend the work of Cook (2011) and also that of Hipsey et al. (2010). The modelling will allow extrapolation to longer time scales than the measured data which was used by Cook (2011).

2. METHODS

2.1. Sample Collection

Due to the lake level rise that had occurred since this proposal was first mooted, the samples could not be taken using standard soil physical techniques (McKenzie and Cresswell 2002). Instead after consultation (Drs W. S. Hicks, A. Baker and R.W. Fitzpatrick pers. comm. 2011) samples were collected using a tube auger designed for such sediments. Samples were collected in up to 1.2 m of water (Figure 7).

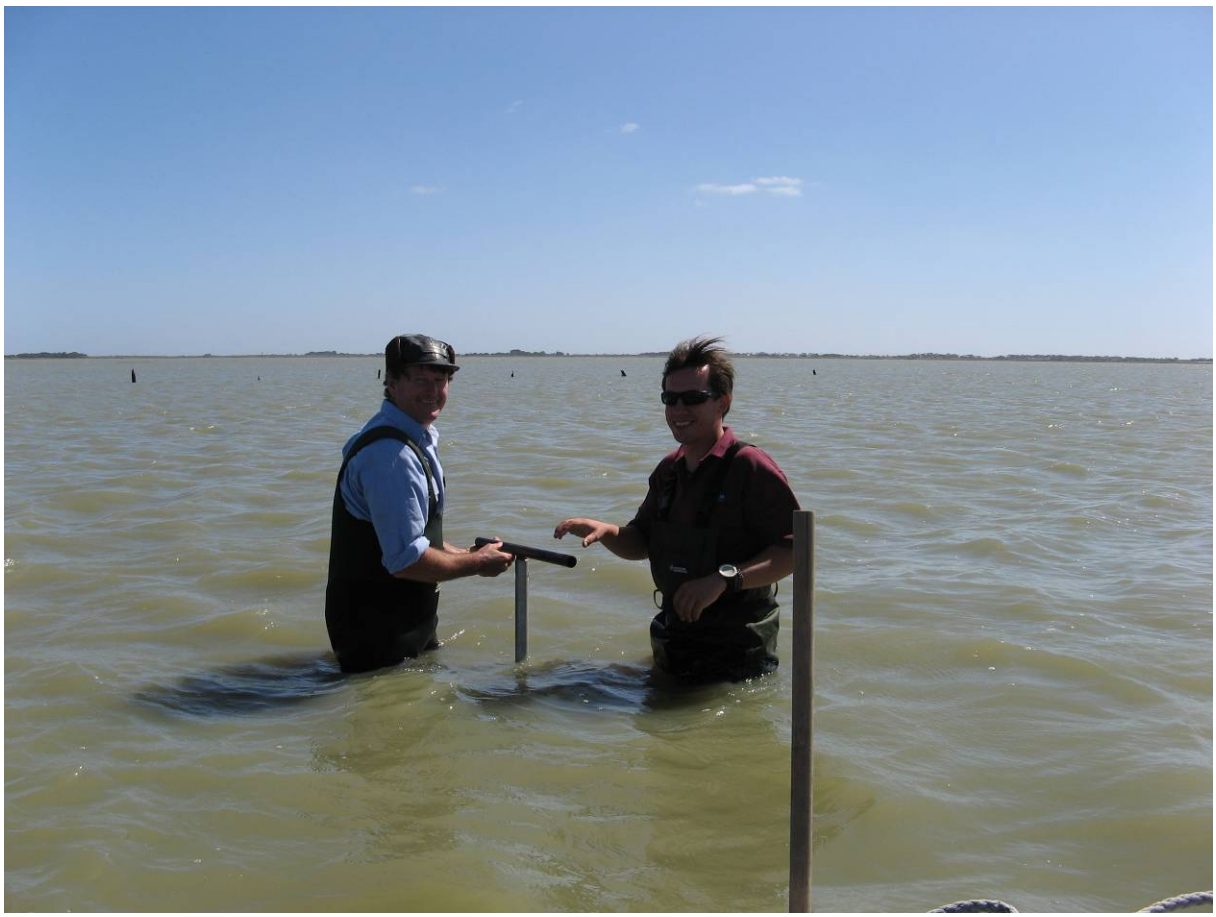

Figure 7. Photo showing sample collection at Campbell Park site.

A sampler especially designed for wet sediments (http://dormersoilsamplers.com/Undisturbed-Wet-Soil-Sampler.html) was used (Figure 8). A number of samples of different lengths were collected from an area of approximately 10 m^2. The longest of these samples was used for the moisture characteristic measurements and bulk density. Cores of approximately 0.4 m in length were used for the diffusivity measurements. A number of other cores were taken (up to 5) for trials for the diffusivity measurements and as bulk samples for particle size analysis and coefficient of linear extensibility (COLE) (McGarry 2002).

Figure 8. Photograph of sampler, showing auger tube, a sample in liner, sample catcher (yellow plastic), plastic liner for sample and cutting shoe. Image from Dormer Engineering.

Samples were collected into a plastic liner and sealed at the ends using duct tape (Figure 9a). These were then transferred to larger plastic tubes and packed in bubble wrap and sealed at the end with urea foam (Figure 9b) before being transported to the laboratory.

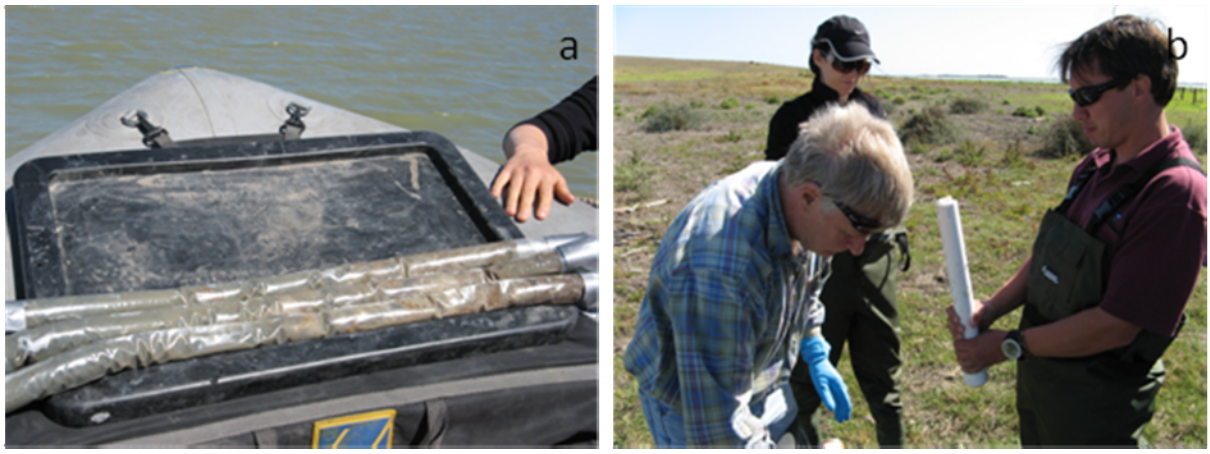

Figure 9. Photographs showing a) samples with duct taped ends and b) tube used for storage and transport of samples.

2.2. Sites

Samples of sediments were collected at four sites, these sites were chosen to be representative of the sediments presented in both lakes with samples from clayey and sandy sediments, and where other studies had been undertaken. The location of the sites is shown in Table 1. Two of the sites were where previous monitoring had taken place *viz* Point Sturt on Lake Alexandrina, and Campbell Park on Lake Albert. These were both sandy sediment sites. The other two sites were in clayey sediments from Boggy Lake (Lake Alexandrina) and Boggy Creek (Lake Albert).

Table 1. Position of the sampling sites.

Lake	Site and Point	Position		Clayey	Sandy
		Easting	Northing		
Alexandrina	Point Sturt	321206	6070328		x
Albert	Campbell Park	341147	6056627		x
Alexandrina	Boggy Lake	335025	6089233	x	
Albert	Boggy Creek	311134	6065845	x	

3. LABORATORY METHODS

Most of the measurement techniques are standard soil physical measurements, except the diffusivity measurements, and have been adapted to deal with the samples collected with the corer and the soft nature of the sediments.

3.1. Diffusivity measurements

3.1.1. Experimental apparatus

An experimental apparatus similar to that used in Kirby et al. (1998) was constructed. This consists of a thermally insulated box with a tray of saturated $CaCl_2$ in the base which at a temperature of 25°C gives a relative humidity of 29% (CRC 1995) (Figure 10). To maintain

the solution at saturation some undissolved crystals are also in the tray. A mesh floor allows the air within the box to circulate and equilibrate with the $CaCl_2$ solution and a balance with an electronic output is placed on the mesh floor. A thermistor measures the temperature in the box and is switched on and off to maintain the temperature at approximately of 25°C (Figure 12). A small fan is used to continuously circulate air within the box. The signals from the electronic balance, thermistor and switch closures (for on and off of light bulb and fan) are sent to a data-logger which records the data and also controls the temperature via switching the light bulb and fan on and off as required.

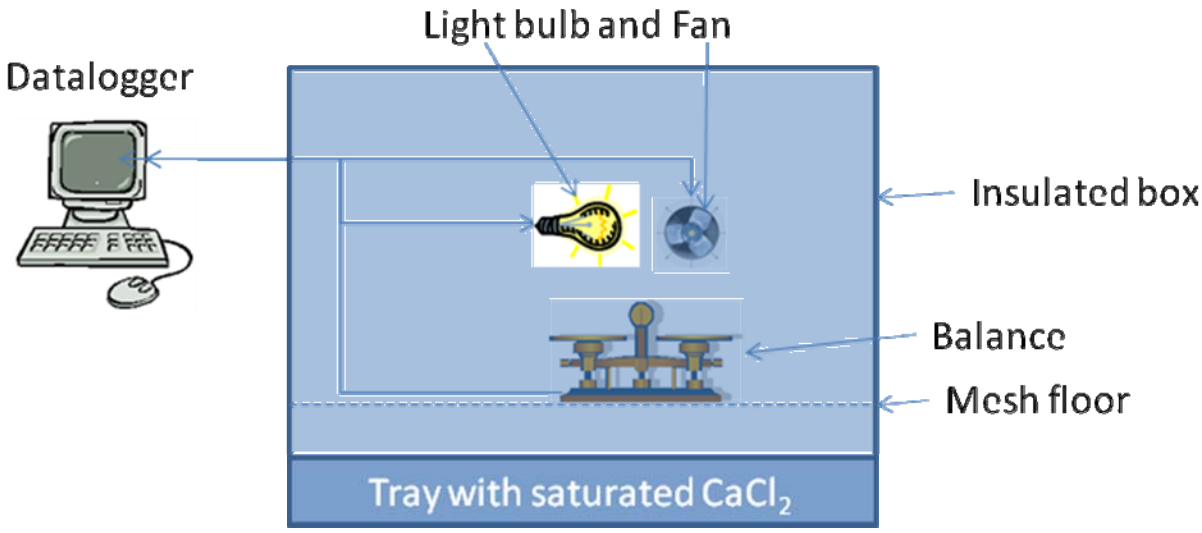

Figure 10. Schematic of experimental apparatus for measuring diffusivity of soil core samples. A thermistor measures the temperature in the box and a light bulb (heat source) is switched on and off to maintain the temperature at approximately 25°C.

A photo of the apparatus is shown with a core on the balance in Figure 11.

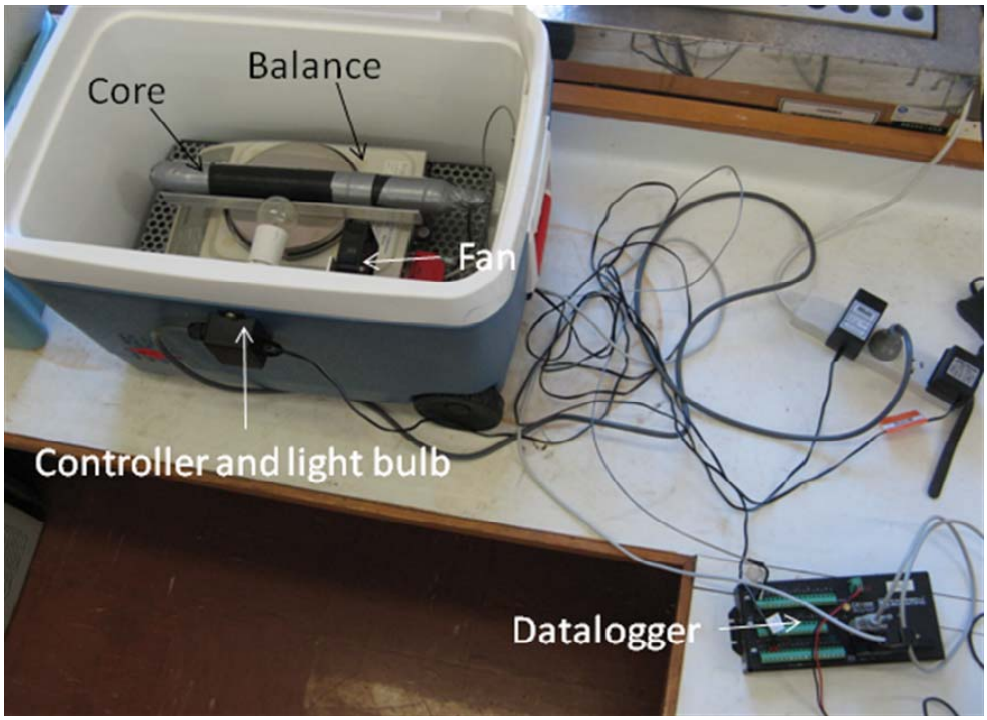

Figure 11. Photo of core in diffusivity apparatus prior to start of test showing the balance, light bulb, mesh floor and data logger. This core had both ends enclosed and to check water loss through the heat shrink plastic.

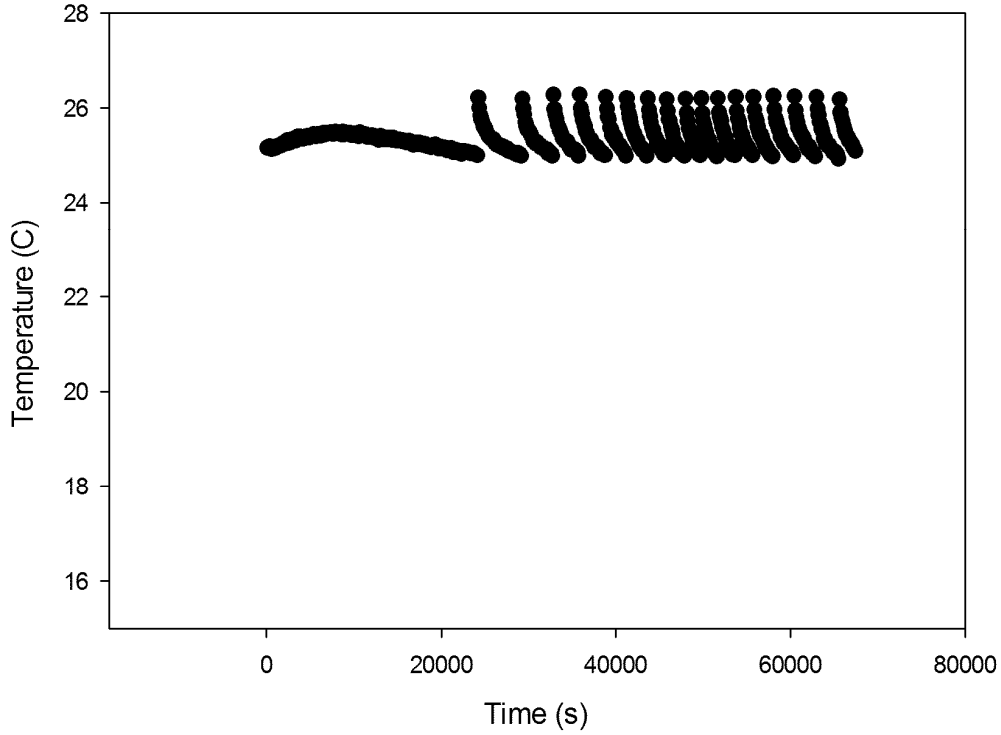

Figure 12. Temperature versus time for box. The initial period before the switching can be seen is due to the box temperature being > 25°C.

3.1.2. Experimental procedure

The cores of soil were unpacked in the laboratory and cores of approximately 0.4 m length chosen for the diffusivity measurements. Some shorter cores were also used in the initial testing of the apparatus. The cores still in their plastic liner were inserted into 40 mm heat shrink plastic and this was shrunk to form a firm fit to the cores. This was done to prevent possible water loss through the sides of the cores. A test with a short core in such a liner with both ends closed with duct tape showed that an insignificant mass loss (< 0.2%) occurred over 6 days (Figure 13).

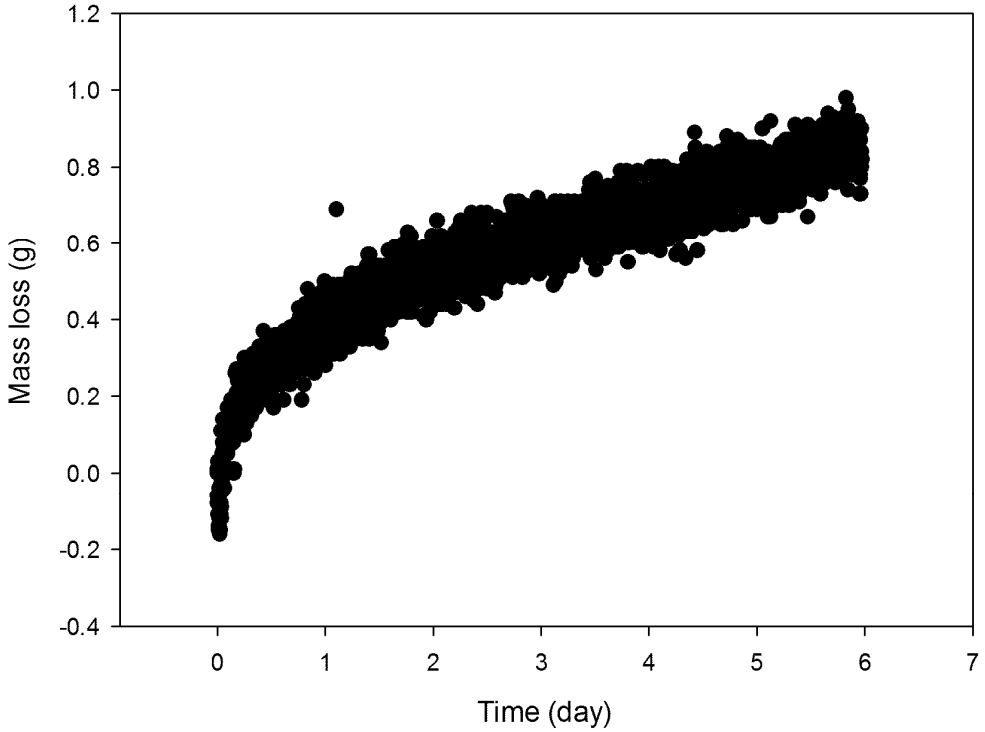

Figure 13. Mass loss from sealed core over a 6 day period.

The cores were then placed in the apparatus with one end exposed. This exposed end is covered by a muslin cloth to prevent the soil slumping. Evaporation occurs from this end of the core. Water will initially evaporate from the core at a rate which is due to the maximum evaporation rate possible (energy limited), and a drying front will move from the exposed surface into the core. As the drying proceeds transmission of water to the exposed end will limit the evaporation rate and this will according to theory decrease linearly with the square root of time. At the end of the drying time the core is quickly removed and sectioned so the water content as a function of distance from the exposed face can be obtained (Figure 14).

Figure 14. Cutting up sequence for core upon removal from the diffusivity apparatus: a) prior to sectioning; b) first few samples sectioned, c) about half of core sectioned and d) cores after oven drying.

The tare mass ($M(0)$ (kg)) and start time were reset to be from the start of the break in the curve. The evaporation since the start time was calculated by:

$$E = \frac{\left(M(0) - M(t)\right)}{1000\rho_w \pi r^2} \tag{1}$$

where $M(t)$ (kg) is the mass at time, t (s), ρ_w is the density of water at the box temperature and r is the radius of the exposed end of the core. The maximum evaporation (*Em*) rate during stage 1 drying was determined from linear regression of E with t (Figure 16) and these values used for inverse modelling (Eching et al. 1994) with HYDRUS1D to obtain the saturated hydraulic conductivity (K_s).

3.1.3. Theory and analysis

The unsaturated flow of water horizontally (gravity does not influence flow) soil can be written as:

$$\frac{d\theta}{dt} = -K\frac{\partial\psi}{\partial x} = -D\frac{\partial\theta}{\partial x} \tag{2}$$

where t is time (s) K is the hydraulic conductivity (m s^{-1}), ψ is the matric potential (m), x is horizontal distance (m), $D = Kd\psi / d\theta$ is the soil water diffusivity (m^2 s^{-1}) and θ is the volumetric water content (m^3 m^{-3}). During the second stage of drying the evaporation rate can be described by (Lockington et al. 1994):

$$E_t = \frac{1}{2} D_e t^{-1/2} \tag{3}$$

where E_t is the evaporation rate (m s^{-1}) and D_e is the desorptivity (m $s^{-1/2}$). The cumulative evaporation during the second stage is then given by:

$$E = D_e t^{1/2} \tag{4}$$

Thus D_e can be found from the slope of E versus $t^{1/2}$. The desorptivity is related to the diffusivity for a linear soil by Philip (1969):

$$\int_{\theta_{dry}}^{\theta_{wet}} D(\theta)d\theta = \frac{\pi D_e^2}{4\left(\theta_{wet}-\theta_{dry}\right)^2} = \int_{\psi_{dry}}^{\psi_{wet}} K(\psi)d\psi \tag{5}$$

and for a Green-Ampt type soil by Philip (1973):

$$\int_{\theta_{dry}}^{\theta_{wet}} D(\theta)d\theta = \frac{D_e^2}{2\left(\theta_{wet}-\theta_{dry}\right)^2} = \int_{\psi_{dry}}^{\psi_{wet}} K(\psi)d\psi \tag{6}$$

The core data when it has been sectioned at the end of the experimental run provides data on water content with distance. This data can be transformed with the Boltzmann similarity transform, $\lambda = xt^{-1/2}$ (Boltzmann 1896, cited in Warrick 2003) so that all of the data collapse down onto one functional relationship between θ and λ. When λ is substituted into eqn (2) and solved for drying from a wetted horizontal semi-infinite column the resulting relationship is:

$$D(\theta) = -\frac{1}{2}\frac{d\lambda}{d\theta}\int_{\theta_{dry}}^{\theta} \lambda d\theta \tag{7}$$

From the experimental data (section 4.1.2 Figure 19) it was found that a function of the form:

$$\begin{aligned} \lambda &= -\frac{1}{b}\ln\left(1-S_e\right) \\ S_e &= \frac{\theta-\theta_{dry}}{\theta_{wet}-\theta_{dry}} \end{aligned} \tag{8}$$

fitted the data well. The reduced water content S_e is a useful way of scaling the functions so they can be easily compared. Substituting eqn (8) into eqn (7) and solving gives:

$$D(\theta) = \frac{1-\ln(1-S_e)}{2b^2} \tag{9}$$

The desorptivity can also be obtained from core data as Philip (1969):

$$D_e = -\int_{\theta_{dry}}^{\theta_{wet}} \lambda d\theta = \frac{\theta_{wet}-\theta_{dry}}{b} \tag{10}$$

The value of D_e derived from eqn (10) can be compared with that derived from eqn (4).

3.2. Moisture characteristics

The moisture characteristics of the sediments were made on selected segments from sediment cores of approximately 0.8 m length. The cores were encased in heat shrink plastic to stabilise them and allow the sub-samples to be handled during measurements.

Initially 50 mm long sub-samples were used, but the equilibrium time for these samples was too long given the limited time in which to complete this study. Subsequently 20 mm long sub-samples were taken from the cores at either side of the midpoint of the depth increment. These sub-samples were encased in heat shrink plastic to prevent distortion of the cores when being removed from the pressure plates for weighing (Figure 15). The methods are outlined in more detail in Cresswell (2002).

Figure 15. Pressure plate showing sub-samples and heat shrink liner. Some shrinkage can be seen with some of the samples.

Upon completion of the moisture characteristic measurements the samples were oven dried and the bulk density determined. The volumetric water content was calculated and the relationship between the matric potential (ψ (m)) and the water content determined by fitting the data to van Genuchten's (van Genuchten 1980) equation (eqn (11)) using RETC (Van Genuchten et al. 1991).

$$S_e = \frac{\theta_s - \theta}{\theta_s - \theta_r} = \frac{1}{\left[1 + |\alpha\psi|^n\right]^m} \qquad (11)$$

where θ_r is the residual water content ($m^3\ m^{-3}$) at which liquid water is deemed to have ceased moving, α is a parameter related to the air entry potential of the soil (m^{-1}), n is a parameter related to the rate of decrease in θ with ψ and m is a parameter related to n and usually taken as $m = 1\text{-}1/n$.

The mean data for each depth was also fitted to the Brooks and Corey (1964) moisture characteristic function:

$$S_e = \left(\frac{\psi}{\psi_i} \right)^{-\beta} \tag{12}$$

where ψ_i (m) is the air-entry potential and β is a shape factor. The capillary length scale (λ_c) can be determined from the parameters in eqn (12) using (White and Sully 1987):

$$\lambda_c = \frac{\psi_i}{3\beta + 1} \tag{13}$$

and compared with other estimates of λ_c.

3.3. Coefficient of Linear Extensibility (COLE)

The coefficient of linear extensibility (Grossman et al. 1968) was measured using a modification of the standard method. The coefficient of linear extensibility (COLE) is a measure of the change in volume of soil or sediments upon drying. This can indicate the likelihood of sediments cracking upon drying. Instead of using clods coated in saran resin, aluminium rings (34 mm internal diameter x 40 mm high) were used to obtain a sub-sample from the sediment cores at various depths. These were then equilibrated at a matric potential of -330 cm of water and the volume of the soil measured ($V_{1/3}$). They were then oven dried to 105°C and the volume determined again (V_{OD}). The COLE was then calculated using (McGarry 2002):

$$COLE = \left(V_{1/3} / V_{OD} \right)^{1/3} - 1 \tag{12}$$

The volume determination was made by using dry sand to fill the space between the shrunk core and the aluminium ring. The volume of added sand was determined by pouring the sand from a measuring cylinder and recording the volume difference.

3.4. Particle Size

The particle size of the sediments at selected depths was measured using the method described by Bowman and Hutka (2002). These were put into the size classes used in the Australian standards (Table 2).

Table 2. Particle size range for soil texture using the Australian standard and USDA standard (Cook and Cresswell 2008).

Texture	Australian standard Particle size range (mm)	USDA particle size range (mm)
Coarse sand	0.2-2	
Fine sand	0.02-0.2	Sand 0.05-2
Silt	0.002-0.02	0.05-0.002
Clay	< 0.002	< 0.002

The particle size data can be used to predict the soil hydraulic properties. A review of methods and procedures for such predictions is given in Cook and Cresswell (2008).

4. RESULTS

4.1. Diffusivity experiments

4.1.1. Desorptivity

The data from the drying of the cores was plotted to determine when the second stage of drying had initiated. There appears to be two parts to the initial drying phase, one where the loss occurs at a high rate, which is possibly the loss of some water that flowed from the end of the core and/or the higher surface area of the muslin, and the second, which is the first stage of drying of the core (Figure 16).

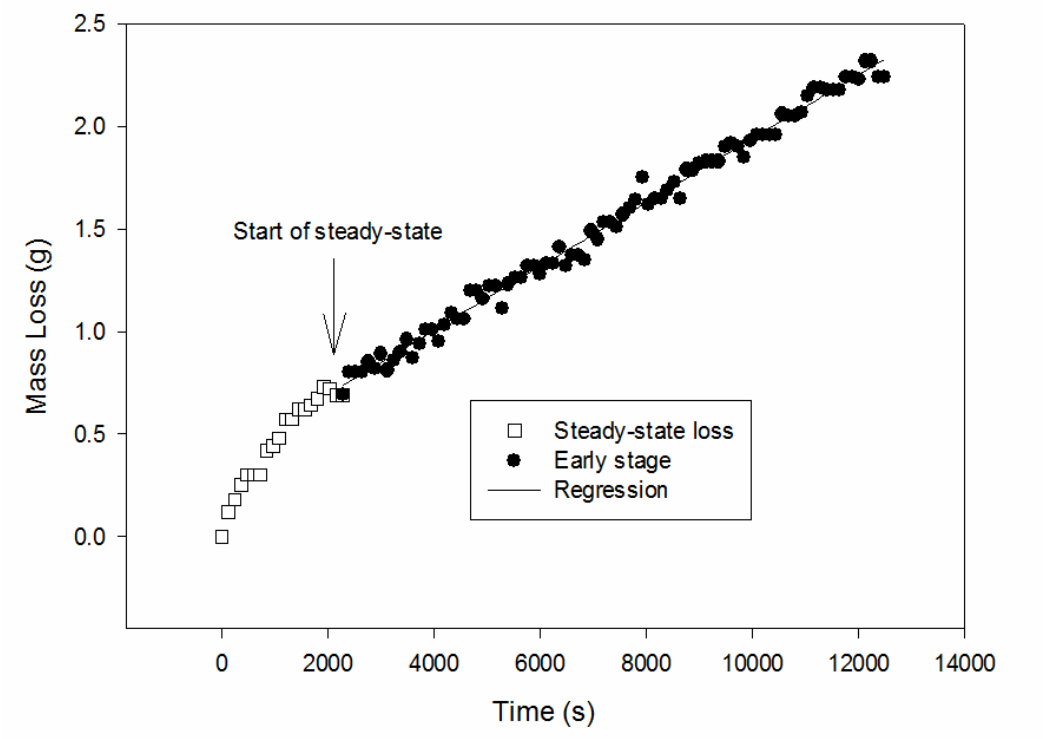

Figure 16. Mass loss from core BL8 in the initial stages of drying. The arrow showing the break in the slope is where it is assumed stage one drying of the core started. The regression shown is used to determine the steady-state and maximum evaporation rate used in the HYDRUS 1D inverse modelling.

From eqn (3) the slope of E versus $t^{1/2}$ is D_e. An example of the drying curve during the second stage of drying is shown in Figure 17 for core PS5.

Table 3. Desorptivity estimates from drying of cores in diffusivity apparatus.

Site and Sample ID	Drying time (day)	Radius at exposed end (mm)	D_e (m $s^{-1/2}$)	*Em* (m s^{-1})	R^2
Boggy Creek					
BC4	4	14.5	8.94×10^{-5}	3.89×10^{-7}	0.995
BC5	6	18.0	7.50×10^{-5}	2.99×10^{-7}	0.995
BC6	12	18.0	9.80×10^{-5}	2.42×10^{-7}	0.999
Mean		16.83	8.75×10^{-5}		0.996
Point Sturt					
PS4	3	16.5	1.07×10^{-4}	2.67×10^{-7}	0.999
PS5	5.6	17.75	9.22×10^{-5}	2.31×10^{-7}	1.000
PS6	7	17.75	1.08×10^{-4}	2.34×10^{-7}	0.999
Mean		17.33	1.02×10^{-4}		0.999
Campbell Park					
CP8	3	15.25	8.03×10^{-5}	2.65×10^{-7}	1.000
CP9	5	15.75	8.36×10^{-5}	2.63×10^{-7}	1.000
CP10	7	15.25	8.23×10^{-5}	2.64×10^{-7}	0.998
Mean		15.42	8.21×10^{-5}		0.999
Boggy Lake					
BL8	4	15.5	8.79×10^{-5}	2.00×10^{-7}	1.000
BL9	6	15.75	7-07 $\times 10^{-5}$	1.64×10^{-7}	1.000
Bl10	10	16.0	8.59×10^{-5}	2.26×10^{-7}	1.000
Mean			7.83×10^{-5}		

Very good fits (R^2>0.99) of the measured data were obtained using eqn (3). The values of D_e were consistent within sites and there was also not much difference between the sites (Table 3). Point Sturt had the greatest value of D_e and Campbell Park the least. However, at the 5% confidence level there is no significant difference for any of the sites.

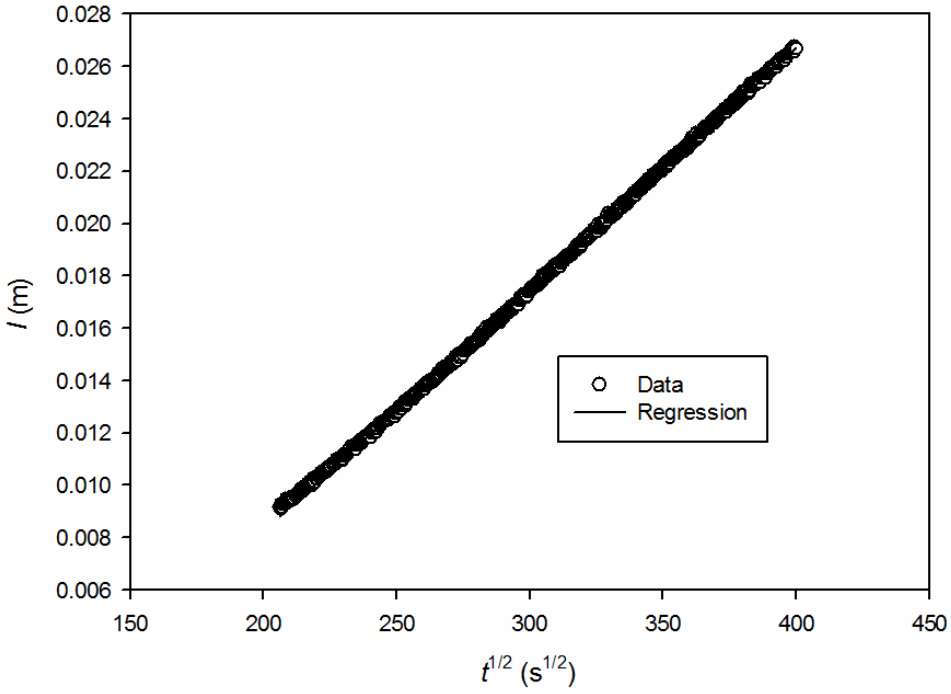

Figure 17. Evaporation (m) versus square root of time ($s^{1/2}$) for core PS5 during the second stage of drying.

4.1.2. Diffusivity

The water content as a function of distance from the exposed face for the Boggy Creek sediments *viz* BC4, BC5 and BC6 shows that especially for BC4 there was some difficulty in determining the water content in the small samples near the exposed end (Figure 18).

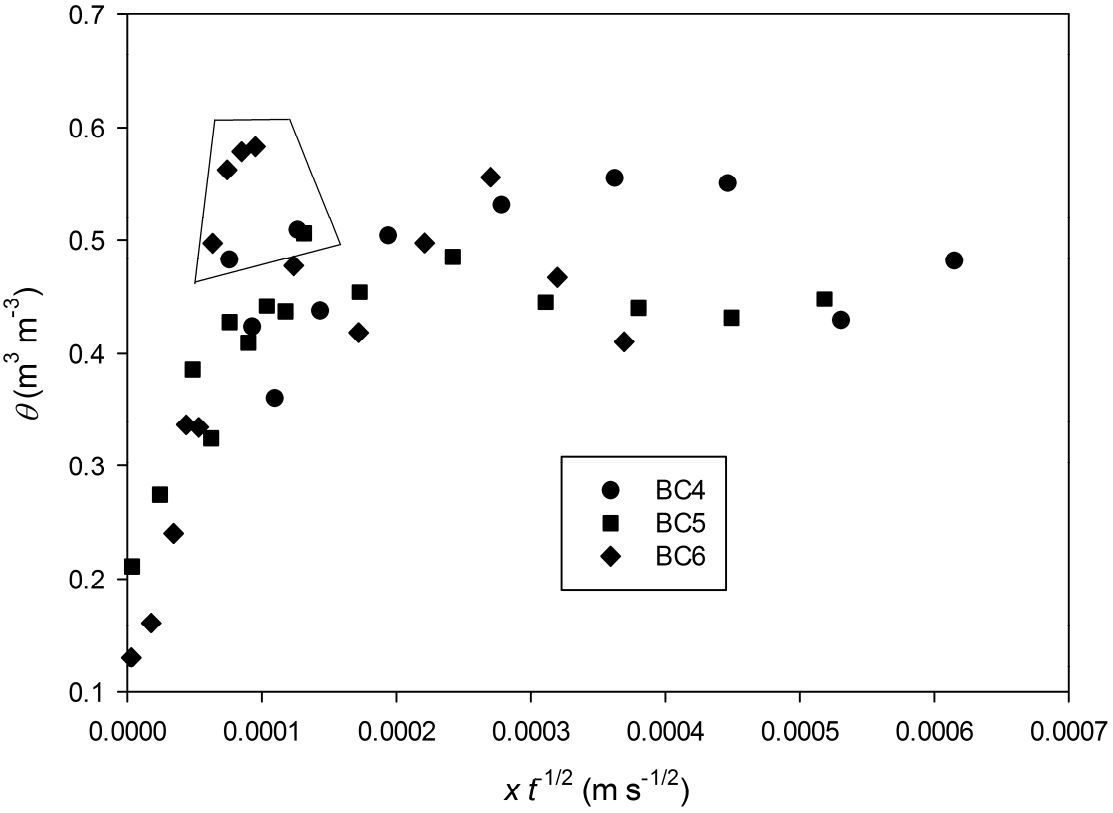

Figure 18. Water content (θ) versus Boltzman transform ($xt^{-1/2}$) for Boggy Creek cores. The data enclosed in the box were removed from the data set as being unreliable when fitting eqn (7).

These values from BC4, three from BC5 and one from BC6 were removed from the data set and then eqn (7) was fitted to the combined data using the least squares regression and the SOLVER function in EXCEL (Figure 19).

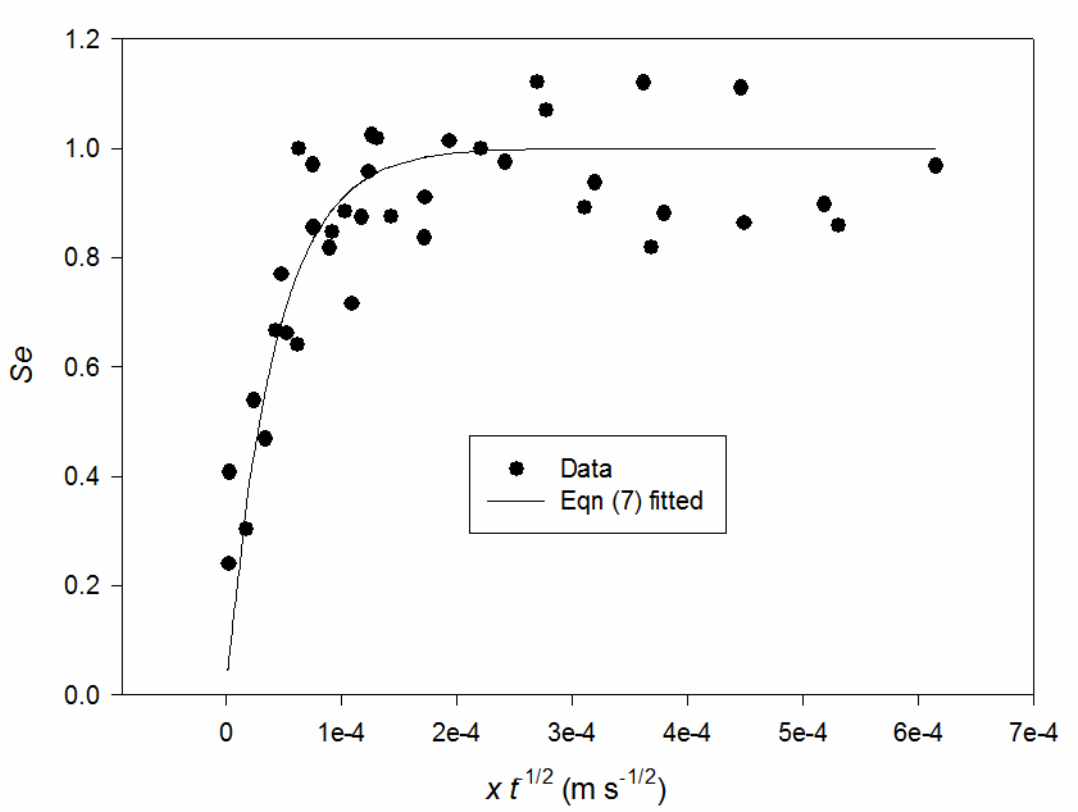

Figure 19. Fit of eqn (7) to experimental data from Boggy Creek diffusivity experiments, with exclusion of data indicated in figure 18.

The coefficients for the best fit (Table 4) are greater than 0.6 for all sediments. The estimate of desorptivity using eqn (9) are similar (Table 4). These estimates of desorptivity are less than the values derived from the mass loss of the cores, with the ratio of D_e:D_e^* ranging from 2.5 for Point Sturt to 4.3 for Boggy Creek. However, given the water content data from the cores is highly variable this difference is to be expected.

Table 4. Parameters derived by fitting eqn (7) to the experimental data for Boggy Creek. The desorptivity estimated from eqn (9) (D_e^*) is also shown.

Site	θ_s (m^3 m^{-3})	θ_0 (m^3 m^{-3})	b ($s^{1/2}m^{-1}$)	D_e^* (m $s^{-1/2}$)	R^2
Boggy Creek	0.498	0.015	23731	2.04 x 10^{-5}	0.77
Point Sturt	0.330	0.001	8153	4.04 x 10^{-5}	0.79
Campbell Park	0.755	0.071	30000	2.28 x 10^{-5}	0.79
Boggy Lake	0.516	0.0	22802	2.26 x 10^{-5}	0.64

The diffusivity as a function of water content shows that the range lies between 1x10^{-9} and 1x10^{-7} m^2 s^{-1} (Figure 20).

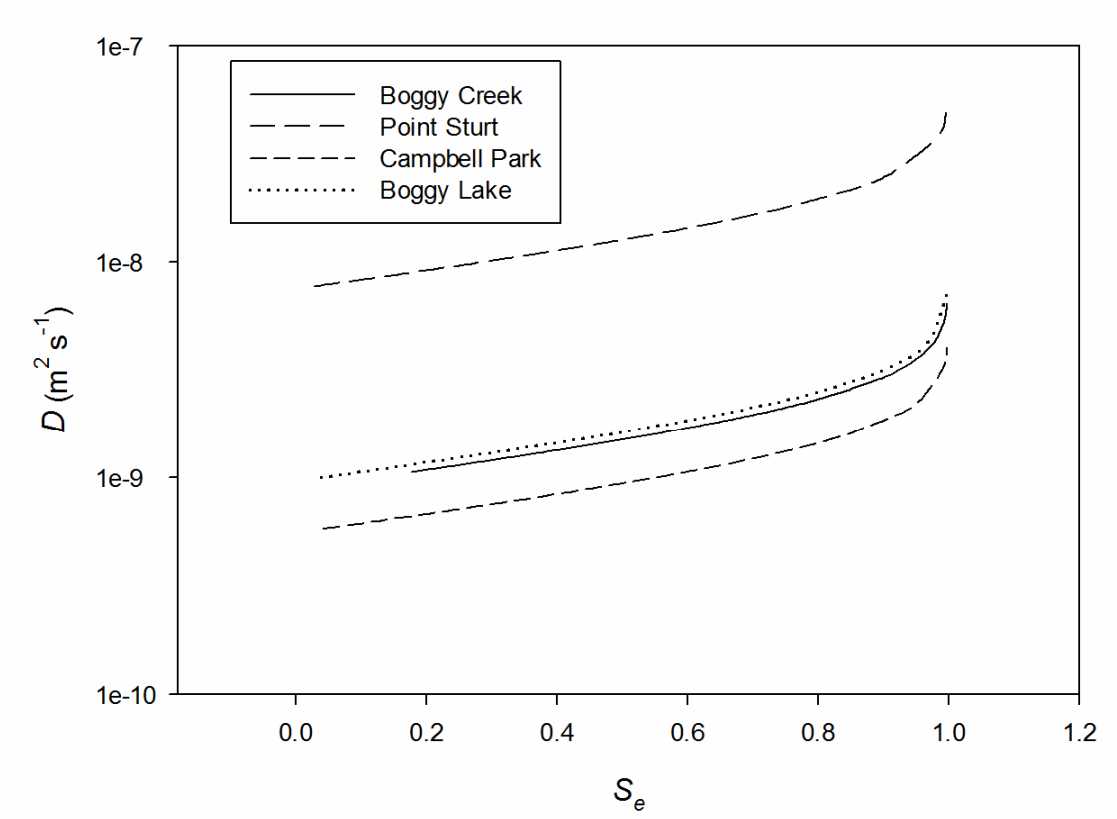

Figure 20. The diffusivity (*D*) as a function of reduced water content (*Se*) for the Boggy Creek site calculated with eqn (8) and the parameter values in Table 4.

The saturated hydraulic conductivity (K_s) can then be estimated from these data using eqns (5) and (6) (Scotter et al. 1978):

$$K_s = \frac{1}{\lambda_s}\int_{\theta_{dry}}^{\theta_{wet}} D d\theta \qquad (12)$$

where λ_s is the macroscopic length scale (White and Sully 1987). This value of K_s can be used to scale the unsaturated hydraulic conductivity function used in the HYDRUS suite of models.

4.1.3. Estimating Saturated Hydraulic Conductivity (K_s) from the Drying Data

The experimental data obtained from the drying experiments can be used along with the moisture characteristic data (to provide limits for parameters) to estimate the best set of parameters and obtain an estimate of K_s. This was done using the inverse modelling option in HYDRUS1D. The values of K_s obtained are in the range from 3×10^{-7} to 2×10^{-6} m s^{-1} (1 to 20 mm h^{-1}), which is not a large range in values. The values for K_s were similar for the three replicates at each site while the other properties varied more (Table 5). The other van Genuchten parameters are also obtained in this fitting process. These parameters are similar and lie within the range of values that are estimated from the moisture characteristic data.

Table 5. Estimated van Genuchten parameters and saturated hydraulic conductivity from inverse modelling of diffusivity experiments. The mean values are shown for each site with the standard deviation in brackets.

Site and Sample ID	θ_s (m^3 m^{-3})	θ_r (m^3 m^{-3})	α (m^{-1})	n	K_s (m s^{-1})	R^2
Boggy Creek						
BC4	0.60*	0.070	1.97	1.953	$2.50x10^{-7}$	0.998
BC5	0.60*	0.079	2.44	1.924	$3.44x10^{-7}$	0.999
BC12	0.60*	0.220	1.77	1.926	$3.00x10^{-7}$	0.997
Mean (std dev)	na	0.12(0.08)	2.1(0.3)	1.93(0.02)	$3.0(0.5)x10^{-7}$	0.998
Point Sturt						
PS4	0.43	0.17	5.25	1.497	$2.31x10^{-6}$	0.992
PS5	0.38	0.17	4.02	1.583	$2.10x10^{-6}$	0.990
PS6	0.39	0.17	5.41	1.998	$2.14x10^{-6}$	0.996
Mean (std dev)	0.40(0.03)	0.17(0)	4.9(0.8)	1.7(0.3)	$2.2(0.1)x10^{-6}$	0.993
Campbell Park						
CP8	0.723	0.075	10.5	1.439	$1.53x10^{-6}$	0.989
CP9	0.8	0.076	10.4	1.483	$1.36x10^{-6}$	0.991
Cp10	0.8	0.094	11.2	1.494	$1.58x10^{-6}$	0.978
Mean (std dev)	0.77(0.04)	0.08(0.01)	10.7 (0.4)	1.9(0.1)	$1.5(0.1)x10^{-6}$	0.986
Boggy Lake						
BL8	0.70	0.037	4.05	1.330	7.9×10^{-7}	0.989
BL9	0.70	0.019	5.50	1.326	8.5×10^{-7}	0.985
BL10	0.70	0	4.16	1.330	1.1×10^{-6}	0.991
Mean (std dev)	0.70(0)	0.02(0.02)	4.57	1.330(0.002)	$9.2(1.8) \times 10^{-7}$	0.986

The hydraulic conductivities for the Boggy Creek and Point Sturt soils presented here (Table 5) are generally an order of magnitude greater than the seepage rates found by Hicks et al. (2009). This is probably due to the different boundary conditions that were imposed by the mesocosms in the Hicks et al. (2009) study. However, variation of over an order of magnitude in saturated hydraulic conductivity is not uncommon.

4.2. Moisture Characteristics

The moisture characteristics were measured and the volumetric water content (θ) determined at fixed values of the matric potential (ψ). The values were determined for three depth increments *viz*; 0-0.1, 0.15-0.25 and 0.35-0.4 m at all sites and also 0.4-0.45 at the Boggy Lake site.

Table 6. van Genuchten's parameters fitted using RETC to the mean, maximum and minimum data sets at each depth increment.

Site	Depth (m)	θ_s (m^3 m^{-3})	θ_r (m^3 m^{-3})	α (m^{-1})	n	R^2
Boggy Creek						
Maximum	0-0.10	0.60	0.10	1.19	1.250	0.996
Mean	0-0.10	0.57	0.20	0.98	1.315	1.000
Minimum	0-0.10	0.56	0.08	0.97	1.401	0.999
Maximum	0.15-0.25	0.58	0.22	1.26	1.445	1.000
Mean	0.15-0.25	0.51	0.12	0.84	1.659	0.998
Minimum	0.15-0.25	0.46	0.07	0.62	1.854	0.997
Maximum	0.35-0.45	0.53	0.09	0.97	1.623	0.980
Mean	0.35-0.45	0.50	0.09	0.80	1.879	0.994
Minimum	0.35-0.45	0.48	0.07	0.77	2.016	0.995
Point Sturt						
Maximum	0-0.10	0.69	0	9.03	1.479	0.993
Mean	0-0.10	0.66	0.01	1.27	1.488	0.998
Minimum	0-0.10	0.46	0.03	3.84	1.840	0.998
Maximum	0.15-0.25	0.53	0.18	1.64	1.540	0.997
Mean	0.15-0.25	0.49	0.10	3.13	1.741	0.998
Minimum	0.15-0.25	0.43	0.02	3.02	2.259	0.997
Maximum	0.35-0.45	0.39	0.08	1.24	1.658	0.996
Mean	0.35-0.45	0.38	0.05	1.64	1.737	0.999
Minimum	0.35-0.45	0.37	0.02	1.74	1.907	0.995
Campbell Park						
Maximum	0-0.10	0.83	0.43	0.76	1.369	0.998
Mean	0-0.10	0.83	0.40	1.46	1.295	0.999
Minimum	0-0.10	0.81	0.29	1.39	1.318	0.996
Maximum	0.15-0.25	0.50	0.09	1.77	1.459	0.999
Mean	0.15-0.25	0.49	0.05	2.31	1.526	0.999
Minimum	0.15-0.25	0.46	0.03	3.15	1.611	0.999
Maximum	0.35-0.45	0.71	0.30	1.11	1.467	0.999
Mean	0.35-0.45	0.63	0.25	1.19	1.610	0.999
Minimum	0.35-0.45	0.51	013	1.19	1.664	0.999
Boggy Lake						
Maximum	0-0.10	0.67	0	0.61	1.118	0.999
Mean	0-0.10	0.65	0.30	1.09	1.259	0.997
Minimum	0-0.10	0.60	0	1.14	1.168	0.998
Maximum	0.15-0.25	0.67	0	0.82	1.161	0.985
Mean	0.15-0.25	0.57	0.08	1.18	1.265	0.999
Minimum	0.15-0.25	0.54	0	1.20	1.276	0.999
Maximum	0.35-0.40	0.72	0.37	1.12	1.315	0.998
Mean	0.35-0.40	0.65	0	1.59	1.139	0.999
Minimum	0.35-0.40	0.58	0	0.51	1.321	0.997
Maximum	0.40-0.45	0.76	0	1.25	1.123	0.996
Mean	0.40-0.45	0.69	0.28	0.95	1.314	0.999
Minimum	0.40-0.45	0.66	0.30	1.30	1.328	0.999

All the data is given in Appendix 1 (Tables 13-16). For each depth increment the mean values of the water content at each potential and the core with the largest water content and

least water content were fitted to the van Genuchten equation (eqn (10)) using the RETC program. The fitted values are shown in Table 6. Some of the variation seen is due to the layering that was observed in the cores with, in particular clayey layers occurring in the Campbell Park cores.

Hicks et al. (2009) obtained similar results with regard to the bulk density and porosity of soils at Boggy Creek and Point Sturt. This suggests that the results presented here may be characteristic of the sediments at these sites.

Table 7. Estimates of capillary length scale (λ_c) using eqn (13) and from field measurements (Cook 2011).

Site and depth (m)	λ_c (m) from moisture characteristics			λ_c (m) from field data
	Maximum	Mean	Minimum	
Boggy Creek				
0-0.10	0.41	0.29	0.25	
0.15-0.15	0.21	0.24	0.35	
0.35-0.45	0.23	0.22	0.21	
Point Sturt				
0-0.10	0.06	0.06	0.07	nd
0.15-0.15	0.17	0.09	0.06	0.21, 0.30
0.35-0.45	0.18	0.14	0.12	0.30, 0.46
Campbell Park				
0-0.10	0.33	0.24	0.17	0.21
0.15-0.15	0.22	0.13	0.10	0.29
0.35-0.45	0.24	0.20	0.19	>0.56
Boggy Lake				
0-0.10	1.04	0.42	0.32	
0.15-0.15	0.35	0.28	0.26	
0.35-0.40	0.37	0.31	0.85	
0.40-0.45	0.49	0.31	0.25	

The estimates of λ_c from the laboratory measurements are similar to the field measurements (Cook 2011) for the Campbell Park site but generally less for the Point Sturt site (Table 7).

4.3. Coefficient of Linear Extensibility (COLE)

The COLE of the soil was determined on the three replicate cores at each depth at each site. The results show that considerable shrinkage occurs, up to 30% for 0-0.1 m depth at Campbell Park (Figure 21). This is due to there being clay in some of the samples in the top 0.1 m of soil. However, cracking was not observed at this site during the drying of the lakes (Figure 22). The clay layers in these samples are shallow and so substantial cracking is unlikely.

The sandy Point Sturt site has little shrinkage while the more clayey Boggy Creek and Boggy Lake soils show shrinkage down to 0.4 m in depth. These are generally consistent with field observations (Figures 23, 24 and 25).

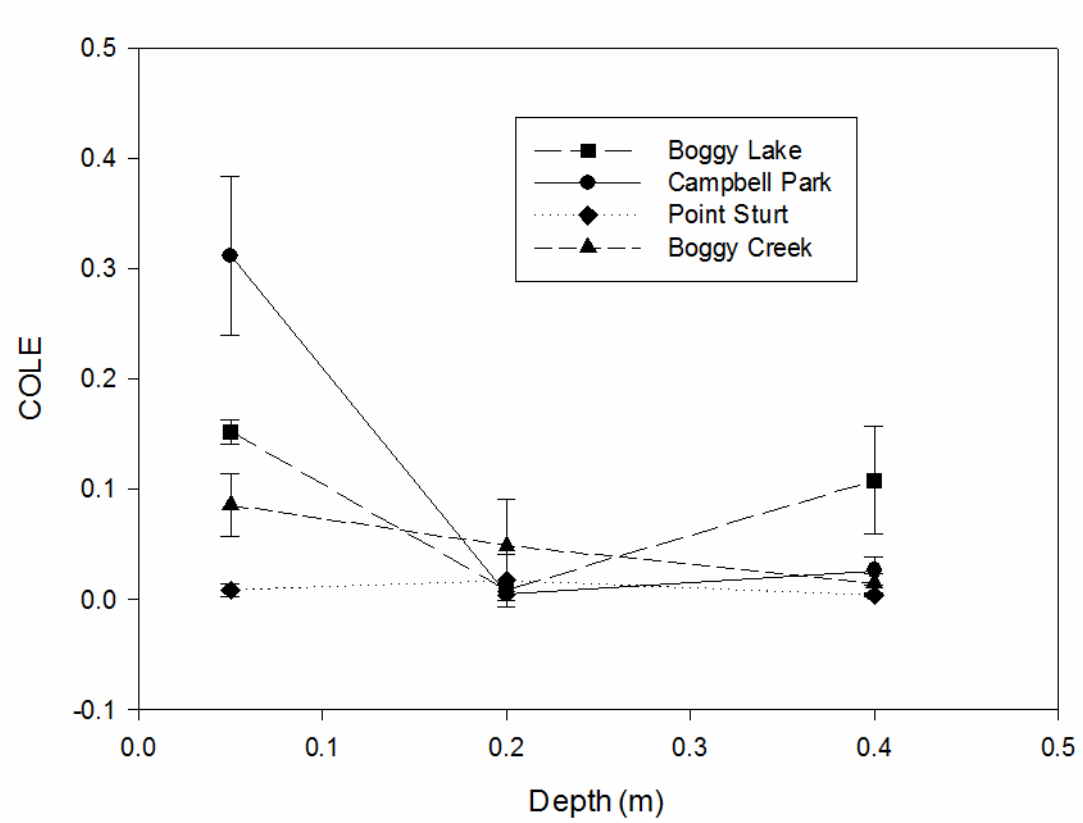

Figure 21. Mean COLE at average depth of sample for all sites. The error bars are the standard deviation of the 3 replicates.

Figure 22. Campbell Park site during piezometer installation showing absence of cracking (from Earth Systems 2008).

Figure 23. Point Sturt site during piezometer installation showing absence of cracking (from Earth Systems 2008).

Figure 24. Boggy Lake under drying illustrating cracking of the surface.

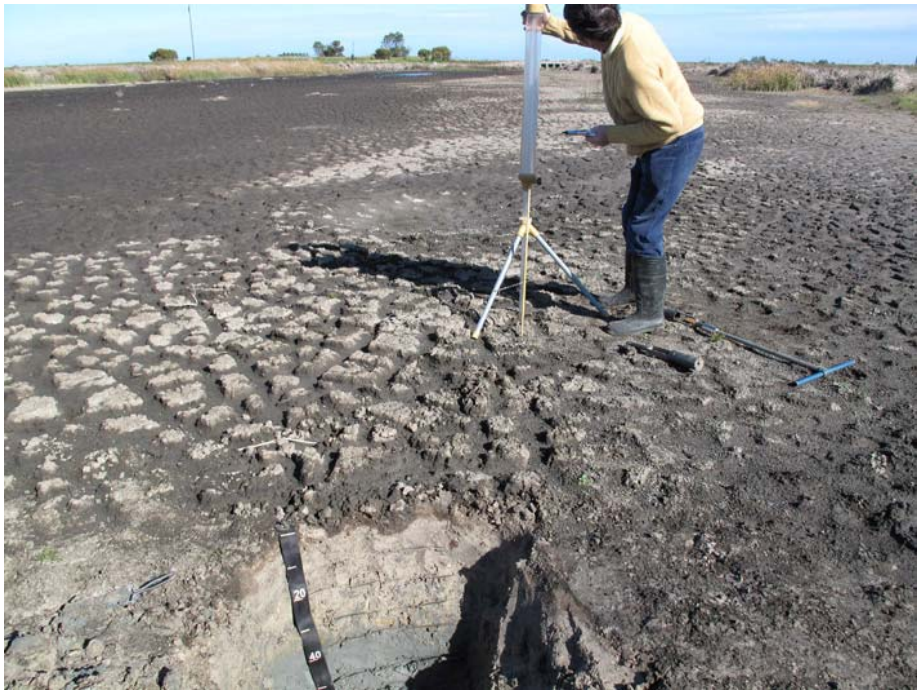

Figure 25. Photograph showing cracking of sediments and infilling at Boggy Creek site. (Photograph by Dr R. W. Fitzpatrick).

4.4. Particle Size Analysis

Samples from the remaining material in the depth increment from which cores were extracted for the moisture characteristic measurements were also analysed for the particle size. These showed that the sediments were mainly dominated by sand or silt sized fractions with only a few samples at the Campbell Park (CP), Boggy Creek (BC) and Boggy Lake sites (BL) with high clay contents (Table 8).

Table 8. Particle size of samples from sediments at Campbell Park (CP), Point Sturt (PS), Boggy Creek (BC) and Boggy Lake (BL). The depth increment and site are in column 1 and texture in column 7.

Site, Sample no. and depth increment	Clay %	Silt %	Fine Sand %	Coarse Sand %	Total Sand %	Texture
CP2 0-10cm	56.05	9.34	27.99	6.61	34.60	Clay
CP2 10-30cm	6.67	0.56	39.74	53.03	92.78	Sand
CP2 30-50cm	11.67	1.11	65.48	21.74	87.22	Sandy Loam
CP3 0-10cm	49.50	16.50	29.60	4.39	33.99	Clay
CP3 10-30cm	5.56	2.22	53.81	38.41	92.22	Sand
CP3 30-50cm	13.33	2.78	71.59	12.30	83.89	Sandy Loam
CP4 0-10cm	57.11	16.58	23.95	2.36	26.31	Clay
CP4 10-30cm	5.49	1.10	57.45	35.96	93.41	Sand
CP4 30-50cm	13.89	2.22	71.76	12.13	83.89	Sandy Loam
PS1 0-10cm	1.05	0.00	41.25	57.69	98.95	Sand
PS1 10-30cm	2.63	0.00	24.17	73.20	97.37	Sand
PS1 30-50cm	4.21	0.53	31.66	63.60	95.26	Sand
PS2 0-10cm	1.18	0.00	33.15	65.67	98.82	Sand
PS2 10-30cm	5.00	1.67	27.40	65.93	93.33	Sand
PS2 30-50cm	3.89	1.67	29.03	65.41	94.44	Sand
PS3 0-10cm	1.11	0.00	43.22	55.67	98.89	Sand
PS3 10-30cm	3.89	0.56	22.26	73.30	95.56	Sand
PS3 30-50cm	2.78	1.67	40.62	54.93	95.56	Sand
BC1 0-10cm	31.54	10.00	56.06	2.40	58.46	Clay Loam
BC1 10-30cm	15.71	1.43	80.53	2.33	82.86	Sandy Loam
BC1 30-50cm	10.71	1.43	85.36	2.50	87.86	Sandy Loam
BC2 0-10cm	28.62	6.96	62.68	1.75	64.42	Clay Loam
BC2 10-30cm	12.84	2.70	81.81	2.65	84.46	Sandy Loam
BC2 30-50cm	10.42	2.08	83.13	4.38	87.50	Sandy Loam
BC3 0-10cm	19.61	9.05	69.55	1.79	71.34	Loam
BC3 10-30cm	10.71	2.14	84.90	2.24	87.14	Sandy Loam
BC3 30-50cm	9.29	2.14	85.43	3.14	88.57	Sandy Loam
BL1 0-10cm	54.42	16.21	20.91	8.45	29.37	Clay
BL1 10-30cm	19.17	5.83	73.40	1.60	75.00	Sandy Loam
BL1 30-50cm	14.62	4.62	79.71	1.06	80.77	Sandy Loam
BL2 0-10cm	61.45	20.81	17.15	0.59	17.74	Clay
BL2 10-30cm	30.83	10.00	58.30	0.87	59.17	Clay Loam
BL2 30-50cm	22.50	9.17	67.28	1.05	68.33	Clay Loam
BL3 0-10cm	43.65	16.03	38.71	1.60	40.32	Clay
BL3 10-30cm	25.00	10.53	62.89	1.58	64.47	Clay Loam
BL3 30-50cm	26.03	13.01	60.16	0.79	60.96	Clay Loam
BL4 0-10cm	64.17	19.17	15.62	1.05	16.67	Clay
BL4 10-30cm	12.14	3.57	83.37	0.91	84.29	Sandy Loam
BL4 30-50cm	28.57	21.43	49.30	0.70	50.00	Clay Loam
BL1 10-30cm	20.00	5.00	73.43	1.57	75.00	Sandy Clay Loam

Using the data in Table 8 and the method of Saxton et al. (1986) as described by Cook and Cresswell (2008), the hydraulic parameters for the sediments were estimated. The saturated hydraulic conductivity and saturated water contents as well as the range of values shows that the Point Sturt site is different from the others in these values, which is a reflection of the consistently high sand content at this site (Figures 26 and 27).

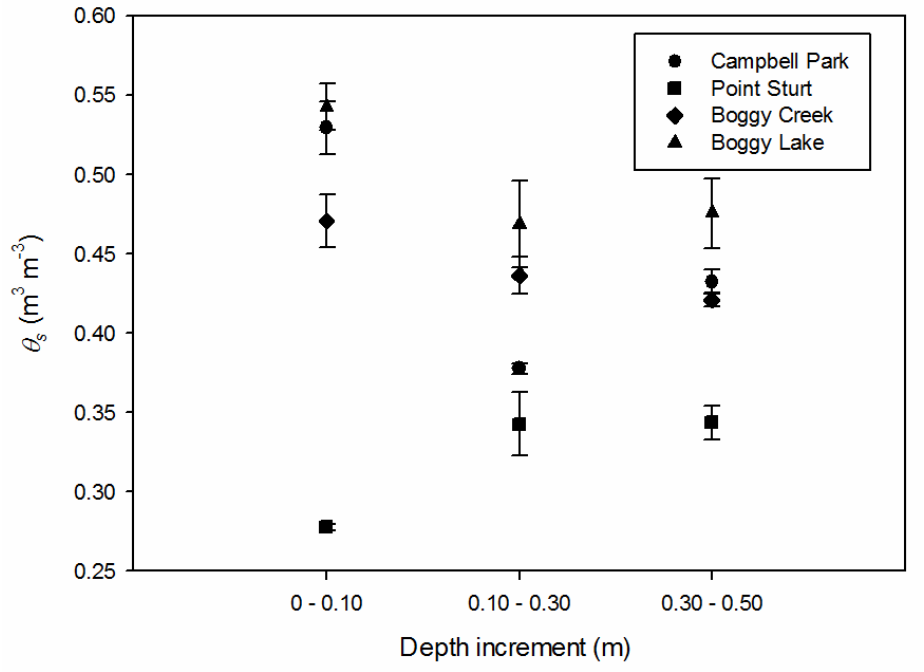

Figure 26. Saturated water content (θ_s) range and mean for the four sites derived from the particle size data using the method of Saxton et al. (1986).

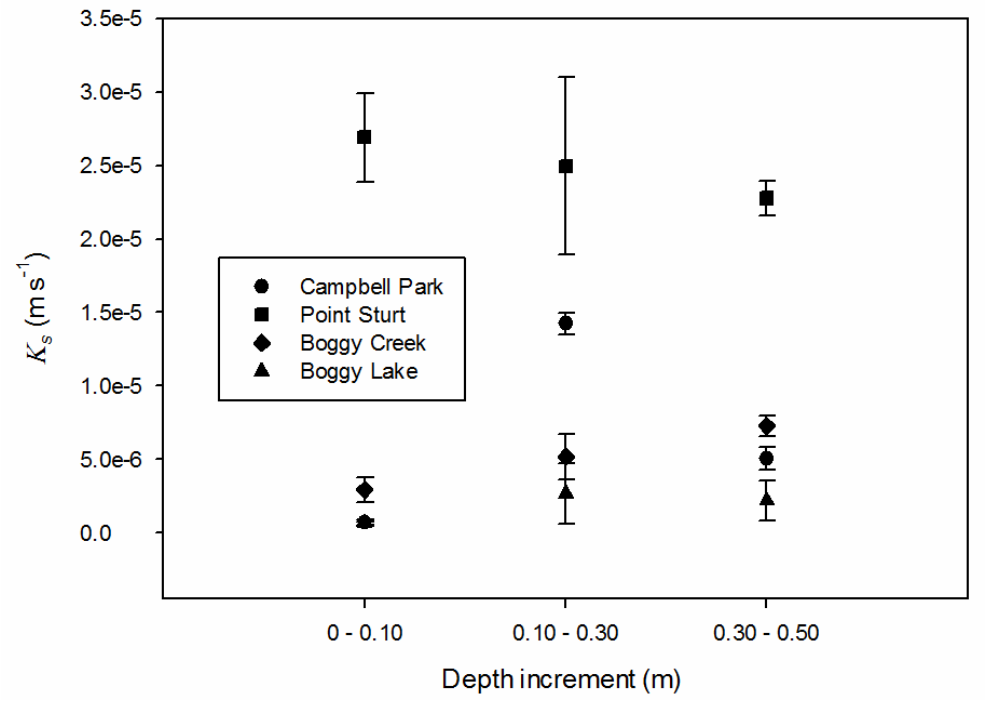

Figure 27. Saturated hydraulic conductivity (K_s) range and mean for the four sites derived from the particle size data using the method of Saxton et al. (1986).

4.5. Numerical Modelling

The modelling of the water and solute transport from the sediment to the lake water was carried out using HYDRUS2D/3D model which solves the Richards water flow and convective transport equations using the finite element method (Šimůnek and Šejna 2007). More details on the HYDRUS2D/3D model and on studies using this software can be found at http://www.pc-progress.com/en/Default.aspx?hydrus-3d.

5. MODELLING

5.1. Comparison of Simulations with Piezometric Head Data

The monitoring data collected by Earth Systems (2010) and used in the first report (Cook 2011) to estimate the fluxes was used as a means to compare the simulations with the observed piezometric height data. This can only be achieved for the Campbell Park and Point Sturt sites as these are the only sites where both sediment samples were collected and piezometric heads were monitored.

5.1.1. Comparison with Point data Using Under Atmospheric Boundary Conditions

The simulation with HYDRUS for Campbell Park using the average soil properties (Table 6) is a reasonable fit to the data (Figure 28). The simulation used rainfall measured at the Narrung measurement station and evaporation data from the Milang meteorological site. Evaporation does not vary greatly spatially, so this data should be representative of evaporation at the Campbell Park site. The simulation does not respond as readily to rainfall input as the piezometric data does. This could be because hysteresis in the soil water properties, the head data for from upslope and the lake are not included, and the soil properties are not measured at the same site. This suggests that the model will successfully model the upper- and mid-slope condition where the lake does not influence the results and during drying.

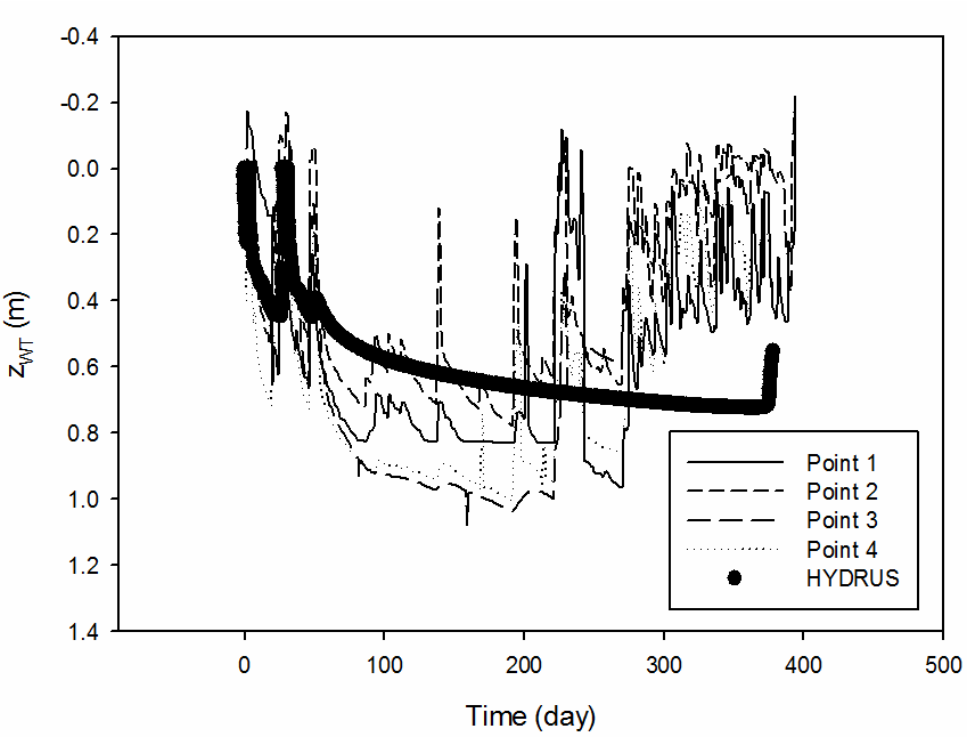

Figure 28. Comparison of HYDRUS2D simulation of water table (z_{WT}) behaviour at the Campbell Park site. The points are the measurement points (Earth Systems 2010) in a transect at this site (see Earth Systems (2010) and Cook (2011) for more details).

We can partially test the effect of the parameter values on the simulations by using the two extreme data sets of soil properties from the measurements and comparing the simulations with the data. The results when simulations with the extreme values are used although more responsive to rewetting do not fit the data as well as the average soil properties (Figure 28). Thus the average soil properties were used in the simulations following for Campbell Park.

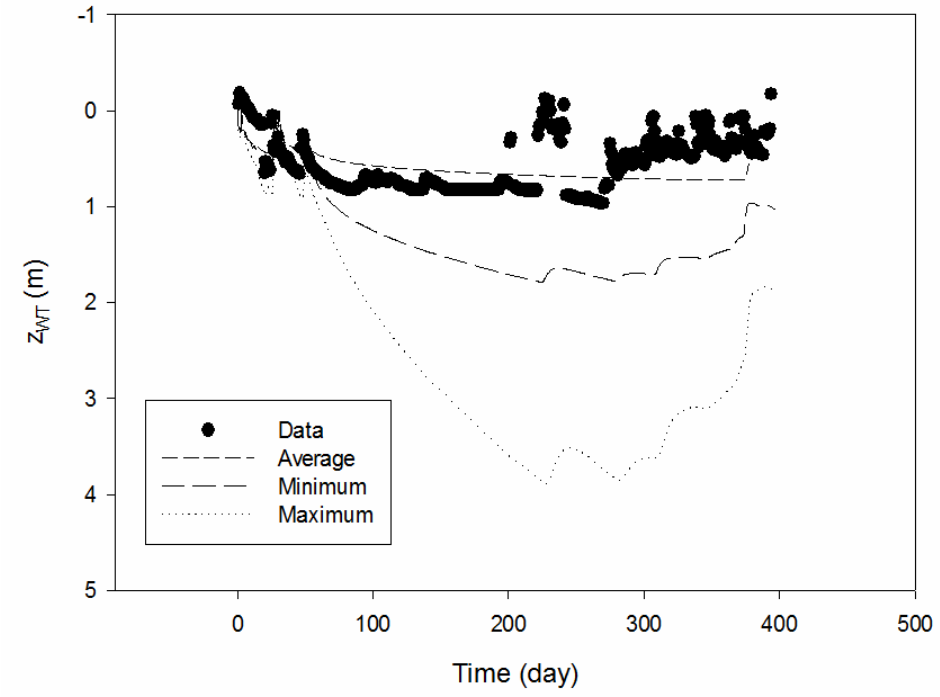

Figure 29. Comparison of simulations with average, minimum and maximum soil properties for the Campbell Park site for the depth of water table below the surface (z_{WT}) with data from point 1 of the piezometer transect.

For the Point Sturt site the simulations show a similar response for points 1 (PS1) and 2 (PS2) but again probably due the lakes influence the simulation rewetting response is later than measured at points 3 (PS3) and 4 (PS4) (Figure 30). The average and maximum soil properties (Table 6) gave a reasonable fit when compared with the other three points in the transect (Figure 31).

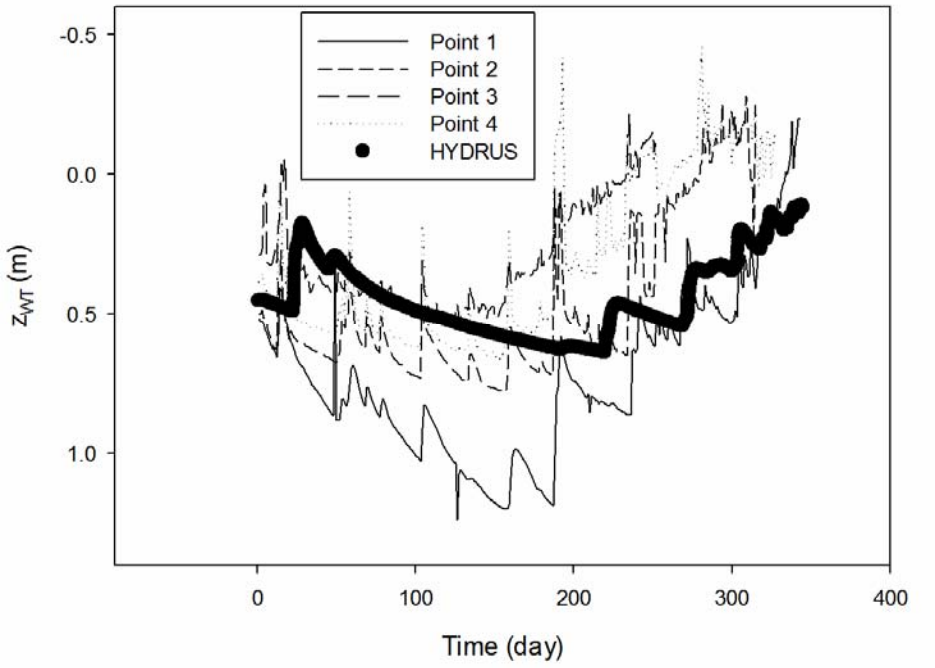

Figure 30. Comparison of HYDRUS2D simulation of water table (z_{WT}) behaviour at the Point Sturt site. The points are the measurement points (Earth Systems 2010) in a transect at this site (see Earth Systems (2010) and Cook (2011) for more details).

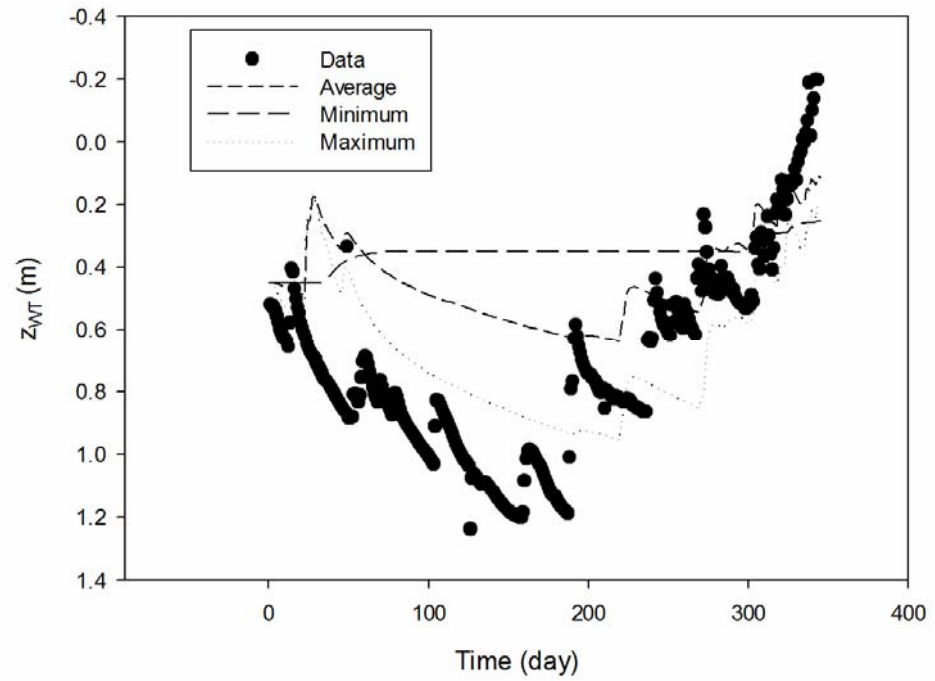

Figure 31. Comparison of simulations with average, minimum and maximum soil properties for the Point Sturt site for the depth of water table below the surface (z_{WT}) with data from point 1 of the piezometer transect.

5.1.2. Comparison with Transects During Drying Phase

In the point simulations no flow was assumed to occur from either upstream or downstream of the piezometer points. To see if including upstream or downstream flow would influence the results, 150 m transects were simulated using HYDRUS2D using the recorded piezometric data at points 1 and 4 as variable pressure head conditions on the side boundaries of the domain. Observation nodes were inserted at the other two monitoring points approximately 50 and 100 m along the transect. Flowing particles were also introduced at node points above the observation nodes to determine the direction of water flow. These flowing particles are transported with the flow of water. These simulations test the hypothesis of Cook (2011) that the water movement would be mainly vertical in the sediments on the basis of the piezometric data.

The simulated heads for points 2 and 3 were almost identical for the Campbell Park site (Figure 32) and only differed briefly around day 5 when the water table height was simulated to be 0.05 m higher at point 3. This suggests that the introduction of the variable head boundary conditions had little effect on the simulated water table behaviour.

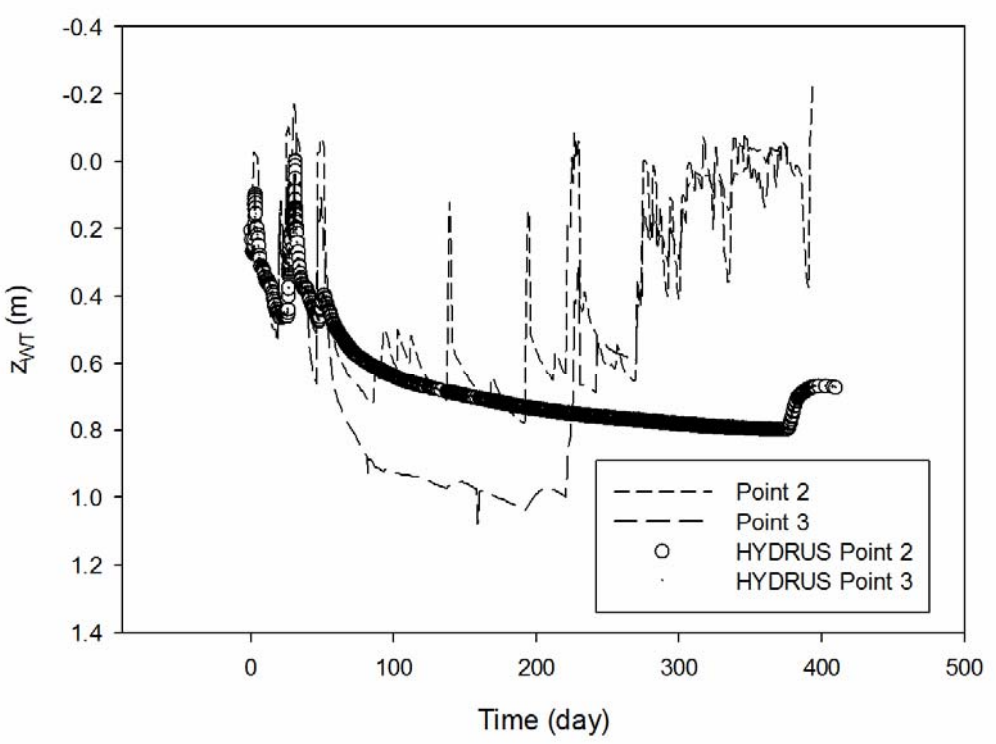

Figure 32. Comparison of the transect simulations of water table height (z_{WT}) simulated for points 2 and 3 with measured piezometric heads for Campbell Park site.

For the Point Sturt site the introduction of a variable head boundary condition using point 1 and 4 piezometric head data has resulted in a delay in the response to rewetting of the sediments for simulated values of z_{WT}. Again there is little difference between the simulations for points 2 and 3 with the maximum difference < 0.06 m (Figure 33). The measured data by comparison shows a difference in the response at the two points. The introduction of the variable head boundaries has not changed the lack of response in the simulations to rewetting of the sediments seen in the piezometric head data after 200 days. This measured differences in z_{WT} may be due to unaccounted variation in the soil properties as the drill cores (Earth Systems 2010) do show different layer at the two points.

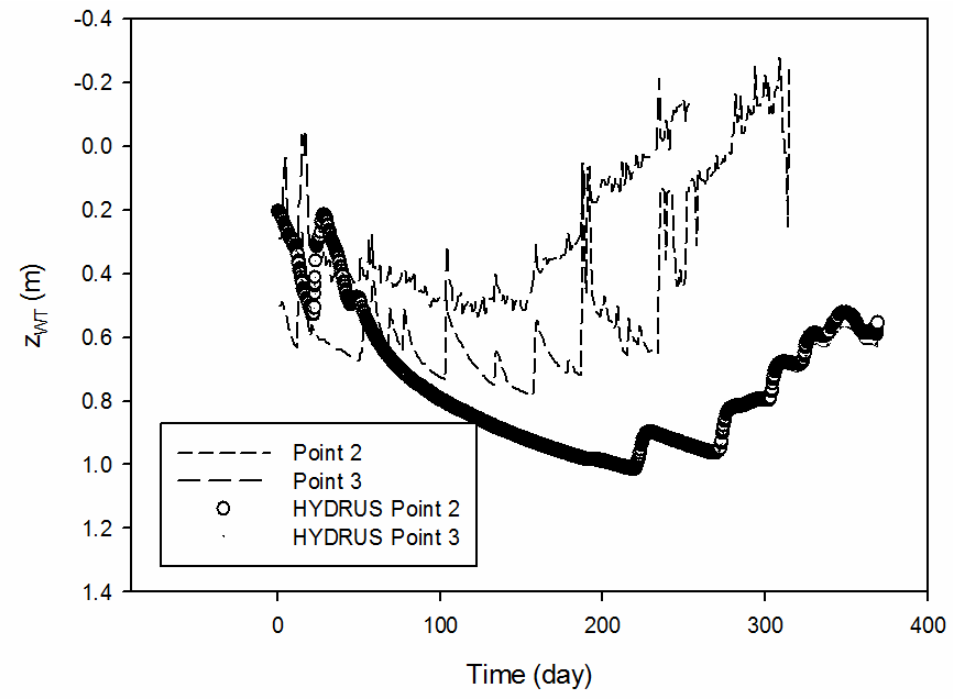

Figure 33. Comparison of the transect simulations of water table height (z_{WT}) simulated for points 2 and 3 with measured piezometric heads for Point Sturt site

The flowing particles showed that the transport of water was essentially vertical at all points and entirely vertical at points 2 and 3 in the Point Sturt simulations (Figure 34a). There was some transport of water downstream at point 1 in the Campbell Park transect (Figure 34b) with the maximum distance of travel being approximately 2 m. These simulations support the contention by Cook (2011) and Hipsey et al. (2010) that the lateral flow of acidity through the sediments will be negligible.

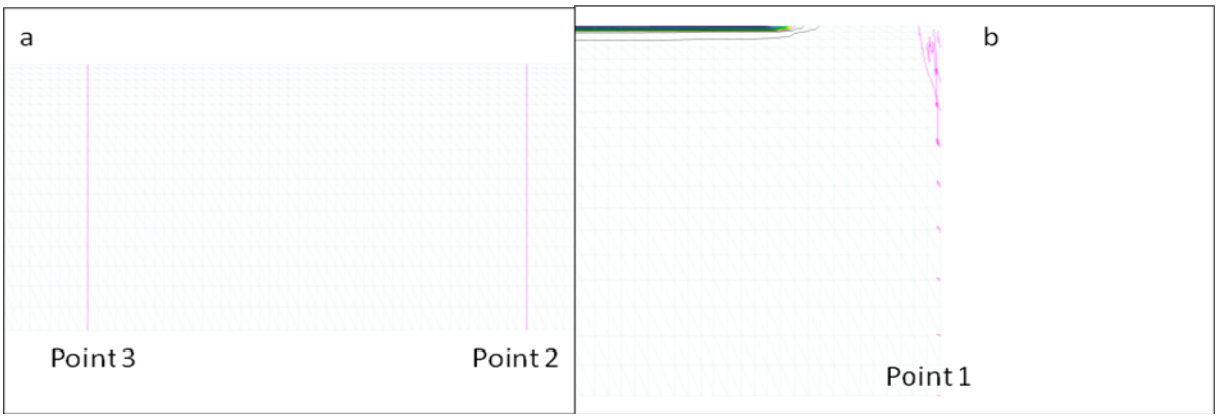

Figure 34. Flowing particle tracks (pink lines) at; a) points 2 and 3 in transect for Point Sturt and b) point 1 in transect at Campbell Park.

5.2. Water transport from the Lake

Simulations using the flowing particle option in HYDRUS2D were performed to see how much the presence of the zero head boundary condition provided by the lake would have on the head upslope. Also using flowing particles the distance water from the lake was likely to travel was computed. A domain 100 m long and 1 m deep were used in the simulations. This domain was sloped towards the lower boundary (lake) using the gradient for each site

previously determined (Cook 2011). The initial conditions were a profile in equilibrium with the head at the lower boundary with the water table at the sediment surface. A surface boundary condition of evaporation at the rate of 4 mm day^{-1} was imposed on the upper boundary, the lower boundary was a no flow condition as was the upper most side boundary. A boundary condition on the lower side boundary (lake) was a constant head with the water table at the surface. The simulation was run for 1000 days.

A typical output near the lake end showing the flowing particle tracks shows that the furthest a particle had travelled in this the Point Sturt sediment was 9.6 m (Figure 35). The particle track maximum travel distances and the distance pressure head influence due to the Lake are shown in Table 9.

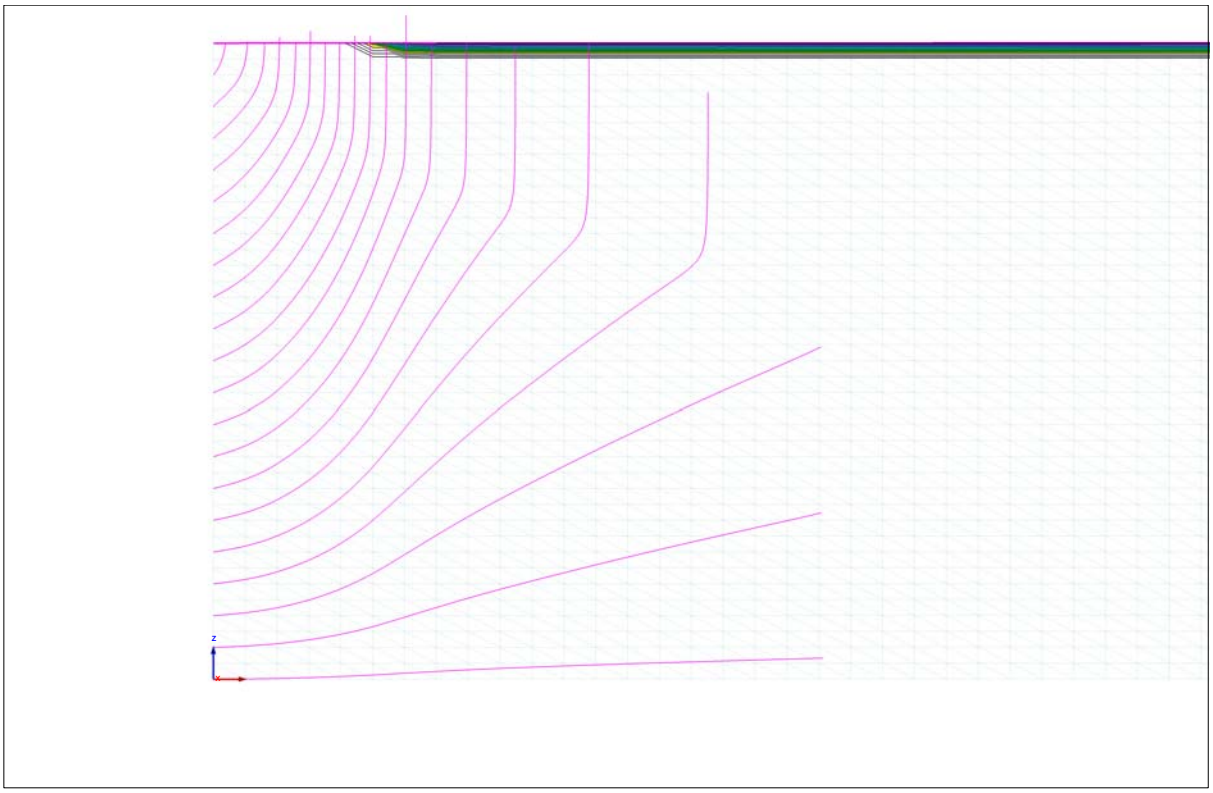

Figure 35. Particle tracks (pink lines) for flowing particles due to water intake at the lake sediment boundary for the Point Sturt sediment with a constant evaporation rate of 4 mm day^{-1}. The horizontal grid cell mesh size is 1.067 m. The particles were initial sited on the outer edge of the domain (left hand edge). The coloured bards at the top beyond 5 m are due to the low potential values caused by drying of the sediments.

In all sites except Point Sturt the pressure head influence is greater than the distance travelled by the flowing particles. This difference for Point Sturt is due to the soil properties of the sediments with greater hydraulic conductivity than the other sites. These results show that transport of alkalinity from the lake to the sediments via groundwater would only have an influence in a margin of < 10 m distance from the shoreline. However, seiching events may have a much larger spatial influence with differences in head of as much as 1 m meaning the influence could be 100s of metres even if only short lived. This may still be of importance in neutralising acidity washed off the exposed sediments during runoff.

Table 9. The estimated distance that the boundary condition imposed by the lake influences water flow from the lakes to the sediments (X_p) and the pressure head (X_h). These distances were calculated after 4 mm day^{-1} of evaporation for 1000 days.

Site	X_p (m)	X_h (m)
Campbell Park	6.5	10.5
Point Sturt	9.6	3.5
Boggy Creek	4.5	8.0
Boggy Lake	5.4	9.4

5.3. Water and Oxygen Penetration into Peds

The water loss and oxygen penetration into peds for the clayey soils that exhibited shrinkage from the COLE measurements (Boggy Creek and Boggy Lake) were simulated using HYDRUS2D/3D. The peds can be considered to be cylinders and so axisymmetric spatial dimensions (radius (r) and depth (z)) can be used. We chose three radii viz 0.05, 0.1 and 0.15 m and two crack depths 0.25 and 0.5 m for a column with a total depth of 1m. The initial condition was chosen as saturation throughout the soil profile and oxygen concentration of zero.

The boundary conditions were chosen as:

- atmospheric on the ped surface and crack length with an evaporation rate of 4 mm day^{-1}, atmospheric oxygen concentration at 20 °C of 0.273 kg m^{-3} and a volatile concentration boundary type,
- no flow at r = 0 (the centre of the ped)
- and a constant pressure of either 0.5 or 1.0 m at the bottom of the ped (z = 1 m).

The oxygen consumption of the sediments was based on the values chosen by Cook and Knight (2003) in their modelling of oxygen transport and the other parameters such as atmospheric concentration, Bunsen Coefficient and the diffusion coefficients in water and air were also taken from the same source. Rigby et al. (2006) showed that the oxygen consumption by pyrite compared to biological sources was small and so this was explicitly calculated.

Table 10. Oxygen penetration depth (z_{O2}) in peds in relation to crack length (z_c), ped radius (r) and water table depth (z_{WT}) at the centre of the ped (r = 0) and at the radius of the column (r = R).

Site	r (m)	z_c (m)	z_{wT} (m)	z_{O2} (r = 0) (m)	z_{O2} (r = R) (m)
Boggy Creek	0.05	0.25	0.5	0.250	0.285
	0.05	0.25	1.0	0.655	0.655
	0.05	0.5	0.5	0.330	0.520
	0.05	0.5	1.0	0.655	0.655
	0.1	0.25	0.5	0.125	0.275
	0.1	0.25	1.0	0.525	0.525
	0.1	0.5	0.5	0.140	0.520
	0.1	0.5	1.0	0.615	0.620
	0.15	0.25	0.5	0.100	0.273
	0.15	0.25	1.0	0.505	0.505
	0.15	0.5	0.5	0.105	0.520
	0.15	0.5	1.0	0.585	0.605
	0	0	0.5	0.06	Na
	0	0	1.0	0.31	Na
Boggy Lake	0.05	0.25	0.5	0.342	0.342
	0.05	0.5	1.0	0.839	0.839
	0.15	0.25	0.5	0.371	0.371
	0.15	0.5	1.0	0.839	0.839
	0	0	0.5	0.124	Na
	0	0	1.0	0.651	Na

The simulations were run for a total time of 1000 days, which was adequate to reach steady-state. This resulted in 12 simulations. All these simulations were run for the Boggy creek data with the average soil properties in Table 6. The hydraulic conductivity was taken from the Table 5 with the mean value used for all layers. Other values of hydraulic conductivity were tried but not shown to change the outcome. Only three of the simulations were run for Boggy Lake sediments that covered the range of variable values. The reason for only running these three simulations is that, the penetration depth was found to be approximately the water table depth in all simulations (Table 10). However, the results in Table 10 will overestimate the penetration depth as the 1000 days with steady-state conditions will represent a worst case scenario. There is a difference in the relationship between the oxygen concentration with depth for the crack surface and centre of the peds (figure 35). This may result in lower acidity concentrations within the peds with radius and depth but more extensive simulations using HYDRUS2D/3D coupled with PHREEQC would be required to determine the extent of the concentration gradient. There would also be value in experiments using columns to determine the acidity distribution. This would take considerably more time to do than is possible in this project. Here we will only concentrate on worse case scenarios.

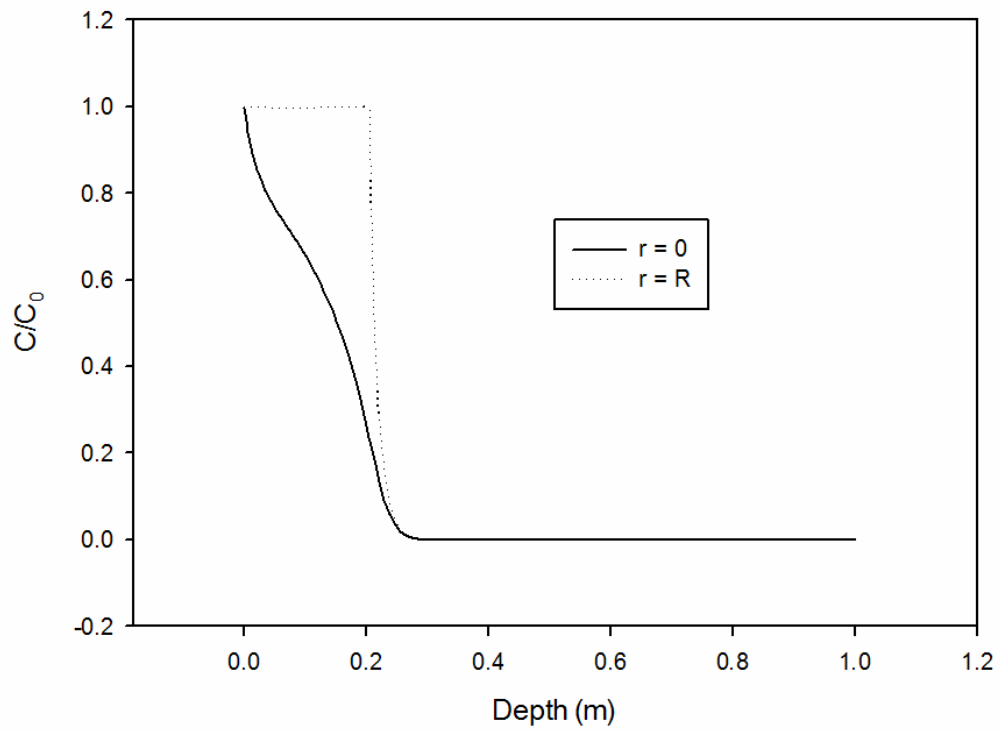

Figure 36. Concentration of oxygen (C) in relation to the maximum concentration (C_0) with depth, at the centre (r = 0) and ped surface (r = R), where R = 0.05 m, the crack length is 0.25 m and the water table is maintained at 0.5 m.

The results indicate that when the water table drops to 1 m below ground level the penetration occurs much more evenly throughout the ped especially when the ped radius is small as for the Boggy Creek sediments. For the Boggy Lake sediments the penetration is even across the sediments. The differences between the Boggy Lake and Boggy Creek sediments with regard to oxygen penetration is due to the physical properties of the sediments especially the higher porosity of the Boggy Lake sediments.

The results indicate similar values although greater penetration of oxygen for the Boggy Lake sediments. Depending on the pyrite concentrations in the sediments at Boggy Lake compared to Boggy Creek this could result in acidity to greater depth and of greater amount in the Boggy Lake sediments.

The cracking and formation of peds substantially increases the oxygen penetration into the sediments and possible acidity generation compared to clayey and sandy sediments with no cracks. This increase in the depth of oxygen penetration can be as great as 500% for the Boggy Creek sediments and greater than 250% for the Boggy Lake sediments. This also suggests that in assessing the acidity of these sediments a careful sampling strategy would have been required to get a correct estimate of the acidity. This is now not possible due to inundation of these sediments. This again highlights the need to have an ongoing process of updating of information through model data integration (Figure 37).

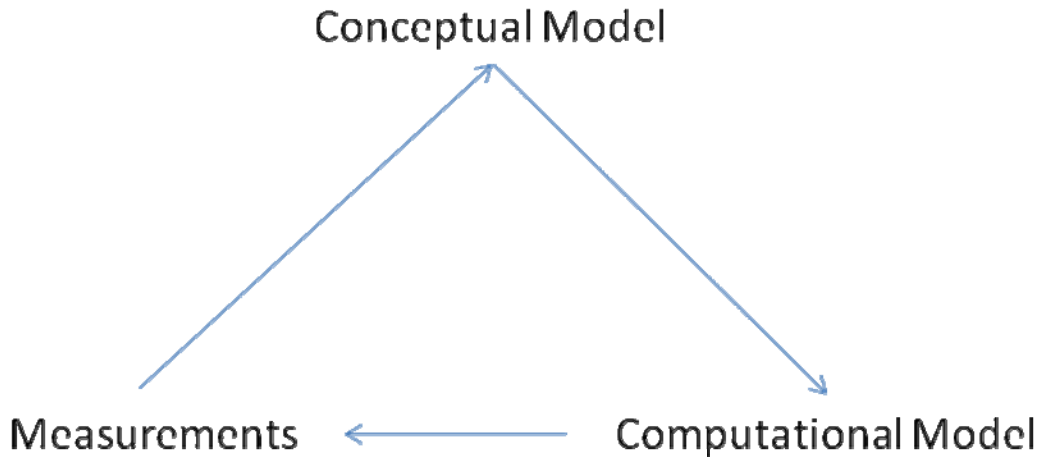

Figure 37. Research strategy for improvement of knowledge.

The more sandy sites Campbell Park and Point Sturt were also simulated using HYDRUS1D to see the depth of oxygen penetration estimated at point 1 (CP1 and PS1) in the transects at these sites using the actual climate data. For Campbell Park the depth of penetration was predicted to be 0.685 m and for Point Sturt 0.300 m. These lie within the range of values in Table 10 for the more clayey sediments. These data were then used when simulating solute losses from these sediment profiles.

5.4. Rewetting of Peds and Solute Transport out of Peds

The peds were rewet using two scenarios which are considered to represent reasonable worst cases. The first considers that the peds are suddenly rewet with the water table rising to the surface but not above the surface and the crack fills to the depth of the crack. The second is where water is also on the surface allowing solute to move out through the upper surface and water to move in.

The water infiltrating the peds is not considered to have acidity or alkalinity associated with it. The oxygen distribution at the end of the drying of the peds is used as the basis for the solute (acid) distribution within the peds. A diffusion coefficient for a passive solute (bromium) of 0.095 cm^2 day^{-1} (Addiscott 1983). The boundary conditions were:

- bottom boundary constant head of 1 m (water table to surface)
- side boundary constant head with head equal to crack depth and linear to zero at surface
- surface either no flux (no water on surface) or constant head of zero (surface inundated)
- no flow boundary conditions on all other boundaries.

The simulations were run for 1000 days and the mass of solute in the domain volume (peds) was obtained from the mass balance information. Examples of the solute distributions prior to and after the 100 days indicate that the solute is pushed towards the centre of the ped and when the surface inundation occurs also down the profile but there is still a concentration gradient towards the top surface (Figures 38 and 39). This diffusion gradient means solute (acidity) will still slowly move into the water body above.

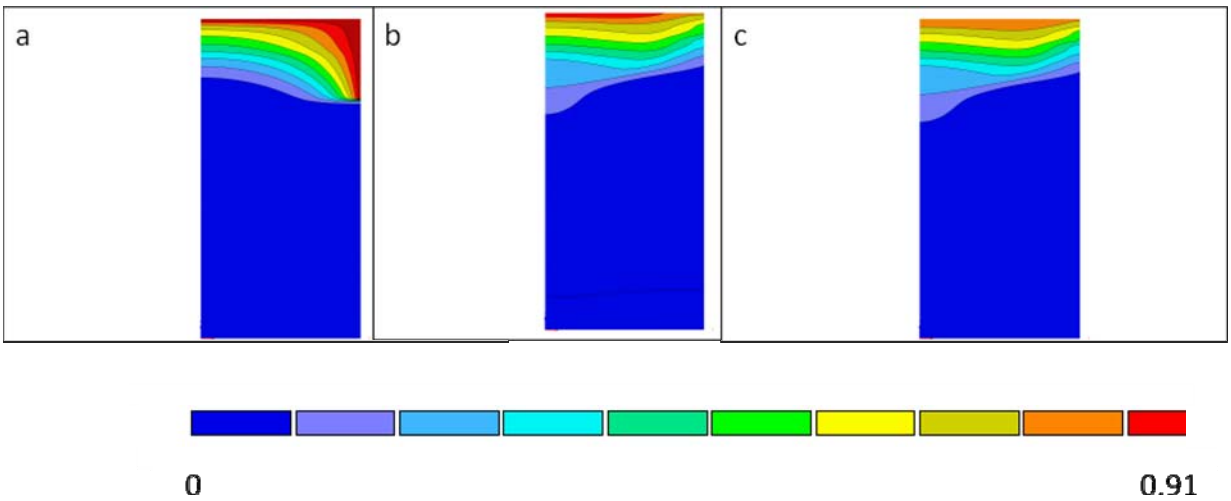

Figure 38. HYDRUS2D simulations of solute transport in peds with radius of 0.05 m, and crack depth on right hand side of 0.25 m and water table depth during drying of 0.5 m for Boggy Creek sediment; a) distribution of oxygen after 1000 of drying, b) distribution of solute after 100 days of rewetting with water only in crack and c) distribution of solute after 100 days of rewetting with water in crack and on the surface. The absolute solute scale is not shown as the scales are different for panel a compared to panels b and c. The scale represents the relative concentration.

The rate of mass lost from the peds shows an initial loss as some of the mass near the constant head boundaries (crack and/or surface) is initially lost but then the loss rate decreases significantly occurs after this (Figure 40). The proportion of mass lost from the peds in relation to ped size, crack depth, drying water table height, and surface boundary condition is shown in Table 11.

Table 11. The proportion of solute mass lost from the peds upon rewetting after 1000 days of water in the crack to the crack depth but not on the sediment surface (M_0) and when water is also on the sediment surface (M_s).

Site	r (m)	z_c (m)	z_{wr} (m)	M_0 (%)	M_s (%)
Boggy Creek	0.05	0.25	0.5	28	28
	0.05	0.25	1.0	33	33
	0.05	0.5	0.5	43	42
	0.05	0.5	1.0	38	38
	0.1	0.25	0.5	33	32
	0.1	0.25	1.0	39	39
	0.1	0.5	0.5	27	28
	0.1	0.5	1.0	44	44
	0.15	0.25	0.5	10	8
	0.15	0.25	1.0	15	14
	0.15	0.5	0.5	13	13
	0.15	0.5	1.0	12	12
	0	0	0.5	13	Na
	0	0	1.0	13	Na
Boggy Lake	0.05	0.25	0.5	57	57
	0.05	0.5	1.0	82	83
	0.15	0.25	0.5	43	43
	0.15	0.5	1.0	48	48

What these results show is that the loss of solute mass from the peds is generally greater than the loss if the surface is flat (i.e. no peds) and can increase the mass loss to up to approximately 30%.

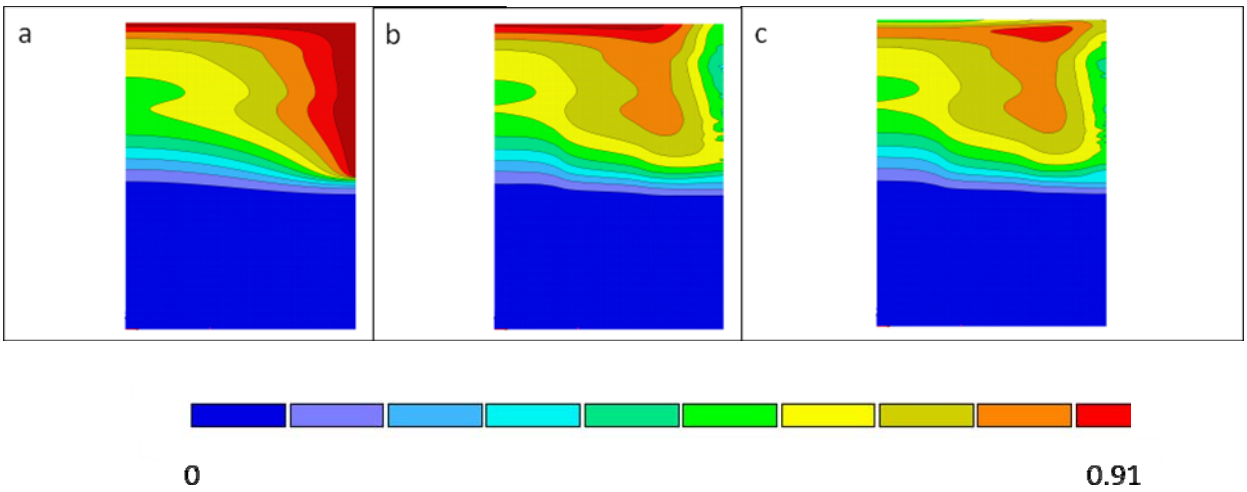

Figure 39. HYDRUS2D simulations of solute transport in peds with radius of 0.15 m, and crack depth on right hand side of 0.50 m and water table depth during drying of 0 m for Boggy Creek sediment; a) distribution of oxygen after 1000 of drying, b) distribution of solute after 100 days of rewetting with water only in crack and c) distribution of solute after 100 days of rewetting with water in crack and on the surface. A relative scale is shown.

The mass loss from peds shows that mass is still being lost at 1000 days albeit slowly from the 0.05 m peds (Figure 40a) compared to the initial loss of solute. The depth of the drying does not make a large difference in the percentage of mass but the depth of the crack does, as this increases the surface area through which mass can be transferred.

There was little difference in the percentage of mass lost between the peds with 0.05 m and 0.1 m radius but the 0.15 m radius showed a reduced percentage loss (figure 40b). The results for the Boggy Lake sediments are greater than those for Boggy Creek with a large initial loss of solute upon rewetting and then very slow loss with time.

The losses from the sandy sediments, Campbell Park and Point Sturt, with no cracks (only loss through the sediment surface) are similar to the losses from Boggy Lake and Boggy Creek when the sediments are cracked (Figure 41). However, the loss from Boggy Lake and Boggy Creek are significantly less than the sandy sites when only loss through the sediment surface is allowed. The rise in the percentage mass lost for the Boggy Lake and Boggy Creek sediments after the initial loss is due to mass balance errors in the simulations even though these are within the mass balance tolerances (5%).

We predict that after the initial loss of solute, upon rewetting of both sandy sediments little further solute loss occurs. This suggests that the acid transport to the lake in the initial stages after rewetting is the most critical point. If the lake is going to acidify then this is likely to occur during this initial rewetting. The clayey sediments where substantial cracking has occurred do pose a further problem as they suggest that further loss of acidity with time can occur from these sites. This would suggest that careful observation and monitoring at such clayey sites may be necessary following rewetting. The flushing of the cracks by wave action could also add to the rate of acidity transfer. Simulation of this scenario was attempted but the computational time was found to be prohibitive. However, the indications were that such intermittent pressure heads would enhance solute loss but not greatly as the solute near the crack had already been lost. These results suggest that initial monitoring following rewetting of the sediments would be adequate in the sandy and non-cracked clayey sediments. However, ongoing monitoring of the cracked clayey sediments is required. The simulations are likely to overestimate this slow release of solute to the surrounding water as slaking and slumping of the peds upon rewetting is likely to fill the cracks and slow the release of solute to the surrounding water. This process of slaking and slumping could also enhance the initial release of solute from the peds. Additional processes that are not taken into account in this solute modelling are cation exchange and precipitation dissolution reactions. Both of these

processes would decrease the solute transport rate as they retard the solute transport. They will also act as a source for the solute and result in solute continuing to be lost with time.

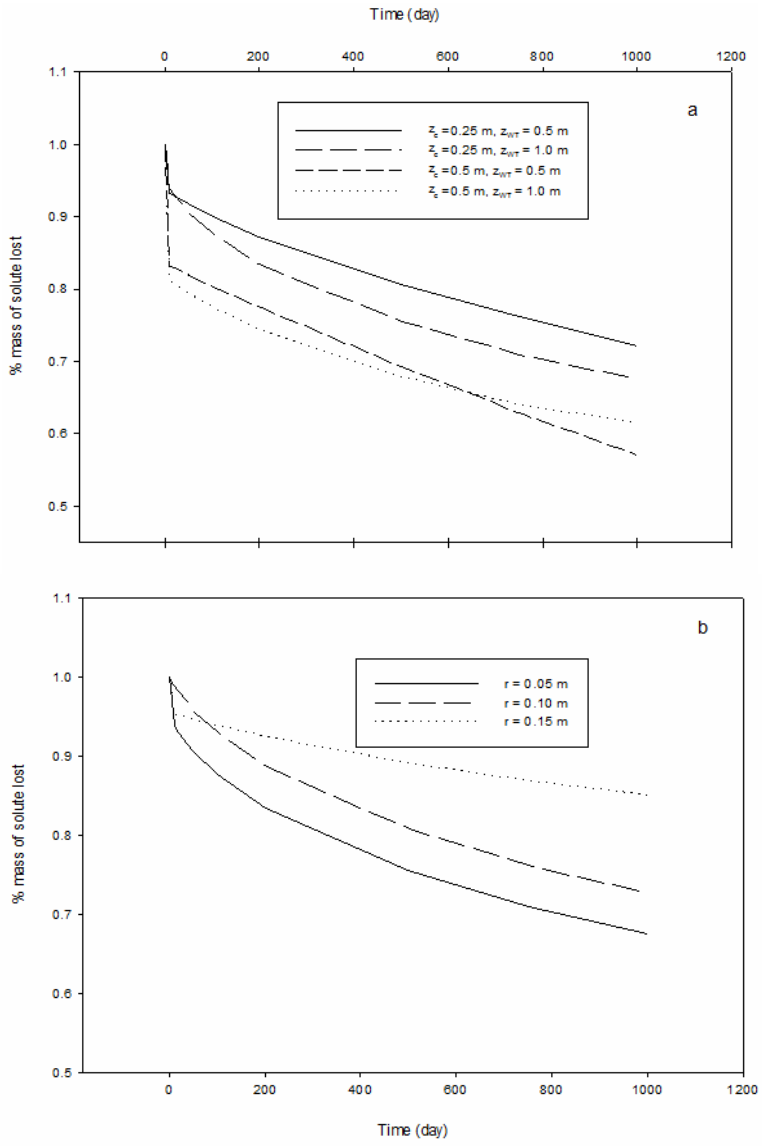

Figure 40. Percentage mass lost with time for peds with; a) radius of 0.05 m and different crack depths and drying water table depths, and b) crack depth of 0.5 m and drying water table depth of 0.5 m and different ped radii. The sediment properties were those from Boggy Creek.

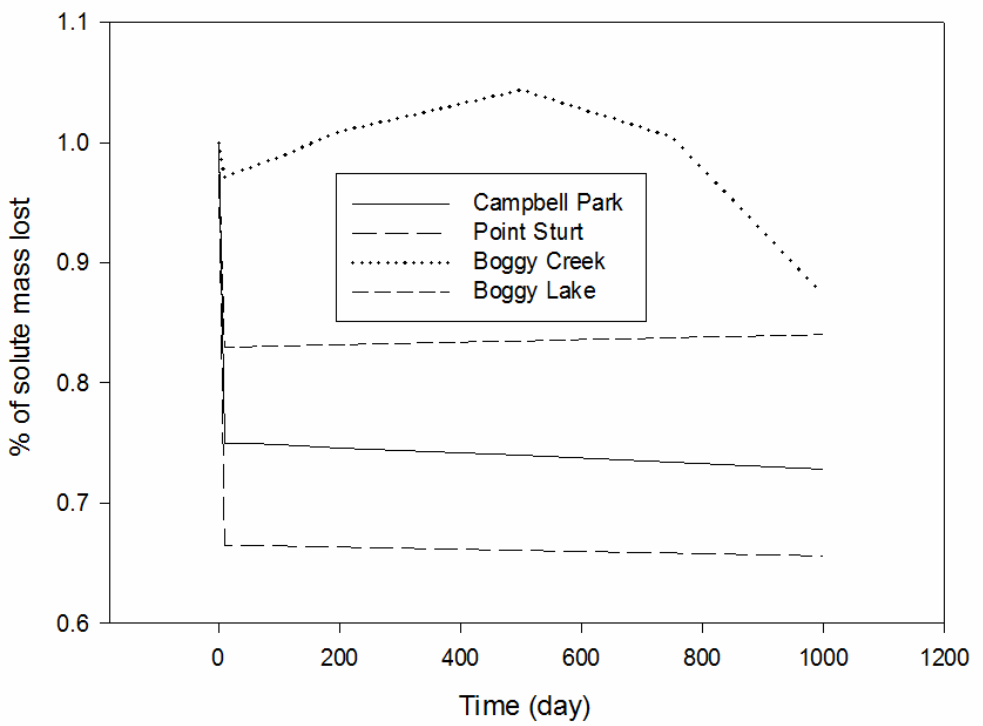

Figure 41. Percentage of solute mass lost with time for sediments inundated with water on the sediment surface following a long period of drying for all four sites.

6. DISCUSSION

6.1. Measurements

The results presented here add a body of knowledge on the physical properties found in sediments of the Lower Lakes. These are valuable as a source of information for use in modelling the behaviour of these sediments and using their response to environmental conditions. We can compare these measured soil physical properties to those inferred from the piezometric and water quality data from the first report (Cook 2011).

Firstly, if we consider the capillary length scale (λ) from piezometer data this was estimated from the air-entry value of the soil (ψ_i) and assuming that the two were equal. The comparison of the field estimates of (ψ_i) and the laboratory measured values are similar for the two sites where this can be compared (Table 12). This assumed that $\lambda = \psi_i$ and implies that $\beta = 0$ (a delta function soil White and Sully (1987)) in eqn (13). However, when the measured value of β is used the capillary length scale is more than halved for the Point Sturt sediments. This would subsequently reduce estimates of the influence of the lake water on the water table from 150 to 30 m (Cook 2011) to between 43 and 8.6 m using the monitoring data. The latter value is in line with the 9.6 m estimated from the modelling (Table 9). Similarly for Campbell Park site values of λ are less from the laboratory data than used in the report of Cook (2011) but the reduction in the estimated influence of the lake water on the water table is 135 m, which is an order of magnitude greater than the influence estimated from the modelling of 10.5 m (Table 9).

Table 12. Comparison of air-entry values from (monitoring data, ψ_{ie}) and laboratory data (ψ_{il}) and capillary length scale (λ) for Point Sturt and Campbell Park sites.

Site	Depth (m)	ψ_{ie} (m)	ψ_{il} (m)	λ (m)
Point Sturt	0.1	Nd	0.13	0.06
	0.2	0.21	0.26	0.09
	0.3	0.30	0.36	0.14
	0.4	0.46	0.36	0.14
Campbell Park	0.1	0.21	0.33	0.23
	0.2	0.29	0.25	0.13
	0.3	> 0.66	0.40	0.2
	0.4	> 0.56	0.40	0.2
	0.5	> 0.46		

The difference could be due to the sediments at the monitoring site having been exposed to drying and consolidation, leading to a much lower total porosity than what was found in the laboratory samples. The maximum water content recorded for the saturated sediments at the Campbell Park site was 0.5 compared to the 0.8 used here (Table 15).

The saturated hydraulic conductivities were determined from the diffusivity experiments and HYDRUS1D inverse modelling and from using the particle size analysis and the method of Saxton et al. (1986). The values obtained were similar. However, these could not be compared with those determined by Earth Systems (2010) as they were measured at different depths.

The shrinkage data showed that the sediments from the two clayey sites had substantial shrinking upon drying. This suggested that considerable cracking of the soil would be possible at these sites and subsequently a model was undertaken that considered the effect of cracking. The sediment in the top 0.1 m depth at Campbell Park also showed moderate cracking but this would be unlikely to generate the cracking that would occur, and was observed at the clayey soil sites. This is backed up by field observations at both sites (Figure 42).

Figure 42. Cracking clays at Boggy Lake rewetted with pH 3 water (Source: EPA)

Due to the flooded conditions the cores taken were of small radius and only represent a small volume. Thus extrapolation of these results to large areas needs to be treated with caution. However, for the Boggy Creek and Point Sturt sites the results are consistent with those of Hicks et al. (2009).

6.2. Modelling

The modelling presented here examines the last mechanism suggested by Cook (2011) as a transport pathway for acidity to get from the sediments to the lake water, i.e. diffusion from the sediments upon rewetting. In order to do this modelling we have firstly tested to see if the model can reproduce the behaviour observed at the monitoring sites. Given the caution noted above about the limited nature of the soil property data, the results for water table head is reasonable and suggested that the model can reproduce the drying behaviour quite well, at the two sites where monitoring data are available.

Significant transport of acidity down slope through the sediments is considered to be unlikely by both Cook (2011) and Hipsey et al. (2010). The results here confirm that this is very unlikely from the particle tracking simulations of the transects. The low slope and hence hydraulic gradients make this mechanism for transport negligible.

These results also suggest that water and pressure heads from the lake do not penetrate very far (<10m) from the lake into the any of the sediments. The exception to this is during lake seiching events where a larger area of the surface sediment may be inundated away from the lake for short durations (hours to few days).

In order to estimate the behaviour of the clayey sediments the penetration of oxygen into them upon drying was estimated. We chose the worst case scenario with continuous drying for 1000 days with at evaporation rate of 10 mm day^{-1}. This showed that a combination of: the water table depth during drying, cracking depth, and ped radius, determines the extent of oxidation of the peds. In particular water table depth of 1 m would result in oxygen penetration to approximately the depth of crack, while a shallower (0.5m) water table depth would limit the extent of oxygen penetration at the centre of the ped. Thus knowledge of the water table depth in such sediments during drying upon exposure will be important in estimating acid generation potential.

Upon rewetting both the peds and the non-cracked sediments immediate release acidity into the surrounding water, which then slows down dramatically. This rapid reduction in acid release is due to advection pushing the acidity (solute) away from the ped crack face and if inundated from the sediment surface also (Figures 38 and 39). This modelling suggests that if the lake does not turn acid upon rewetting of non-cracked sediments then it is unlikely to do so. The exception to this could be localised areas on the lake margins which have limited exchange with the main lake water body. Monitoring data showed that acidification (21.7 km^2 total area) occurred in various locations on the lake margins (Figure 43)

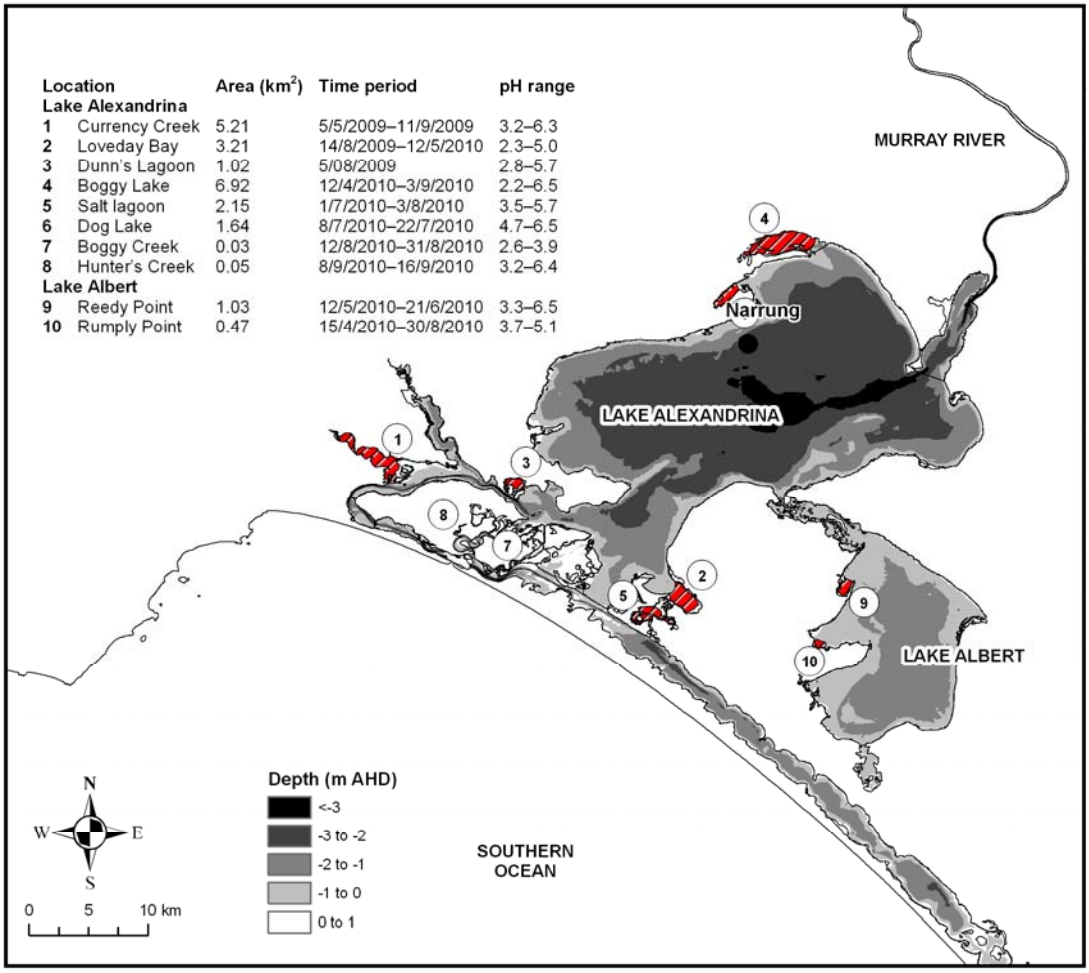

Figure 43. Acidification events recorded in the Lower Lakes from 2007-2010 (Source: EPA).

However, the clayey sediments with cracking are estimated to keep on transporting acidity to the surrounding water for some time to come. These clayey sediments typically also have a higher acidity hazard (Fitzpatrick et al. 2010). Depending on how much alkalinity this water

contains after the initial acidity release for the sediments, some clayey sediments could cause the surrounding water to become acidic for sometime after inundation. This occurred in several locations shown in Figure 43 (Boggy Creek, Boggy Lake and Dunn's lagoon). Despite a connection to the main alkaline lake water body, low pH acidic conditions persisted for a substantial period of time at Boggy Lake with 1000 tonne of limestone used for neutralisation over three aerial dosing events (Figure 43a).

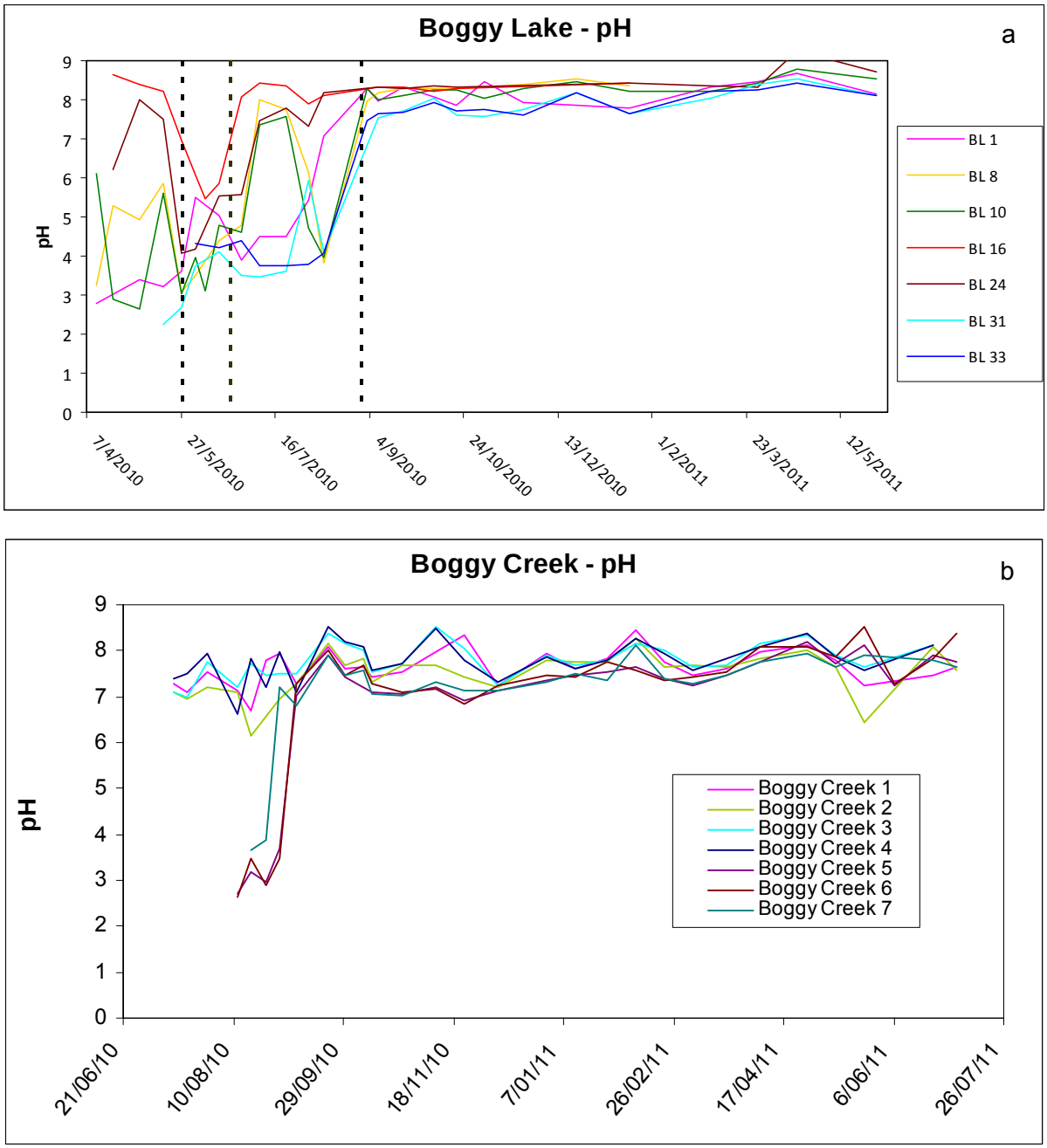

Figure 44. Time course for pH in a) Boggy Lake and b) Boggy Creek following refilling of the lakes. The dashed lines on the Boggy Lake graph indicate when aerial limestone additions to the water body occurred (Source: EPA).

In contrast the Boggy Creek field results show a more rapid neutralisation occurred naturally due to the inflowing lake alkalinity (Figure 43b) which generally supports our findings of lower cracking and acidification potential compared to Boggy Lake. In general the results also show that ongoing monitoring of the water quality in areas where clayey cracked sediments occurred would be sensible. One of the key recommendations of the Lower Lakes acid sulfate soil research program (DENR 2010) that "the exposure of clay-rich sediments in the

deeper inundated regions must be avoided" is also supported by our findings. The South Australian Government strategy to maintain water in Lake Albert via pumping to prevent exposure of clay soils with a high acidity hazard is likely to also have avoided a long-term acidification legacy.

These results are also consistent with the findings from the mesocosm studies of Hicks et al. (2009). They showed that acid release from the Boggy Creek sediments was initially fast and then slowed to a lower rate 7 to 21 days after rewetting. The modelling results show little acid release from the non-cracked sandy sediments once the initial acid release has occurred. The results of Hicks et al. (2009) for their Point Sturt site are consistent with the modelling results, with an initial release and then zero flux of acidity to the surface water (Hicks et al. 2009, Figure 25). The consistency between the modelling results presented here and the experiment results of Hicks et al. (2009), Earth Systems (2010) and EPA field results suggests that the modelling approach taken here has been useful and has offered insights that assist with understanding experimental and monitoring results as well as observations of the Lower Lakes upon drying and rewetting.

There are many more simulations that could be performed given time but what is presented here is considered to be those which have helped to understand the nature of solute transport and hence acid release from these sediments. In particular the rate of sulfate reduction that will occur in the sediments upon rewetting is not addressed here but could be using HYDRUS coupled with PHREEQC. This modelling though would take considerable time to do and require additional validation data to be collected (e.g. use of peepers to study diffusion and cation exchange processes).

7. SUMMARY AND CONCLUSIONS

Sediment samples from both Lakes Alexandrina and Albert were collected in difficult circumstances and transported to the laboratory for a range of soil physical measurements. Due to the time constraints and difficulty obtaining the samples these samples were small radius cores. However, consistent data was obtained from these samples, which has resulted in a body of physical properties for these sediments. This is a valuable source of data and results from these are consistent with monitoring measurements made at two locations each in Lakes Alexandrina and Albert. The results showed the clayey samples to have considerable shrinking capability.

Using these data and the HYDRUS numerical modelling suite of models simulations of the behaviour of these sediments was conducted for a number of scenarios. In particular the effect of cracking and ped formation in the clayey sediments was modelled. This showed that oxidation of these sediments is enhanced by cracking, as is solute release into the surrounding water upon rewetting.

The simulations suggest that an initial rapid release of solute (acidity) is likely. In the cracked sediments further slower release is also likely over time. This suggests that if the lake water does not become acidic upon rewetting then it is unlikely to do so except where cracked clayey sediments occur. The modelling results are consistent with earlier mesocosm experimental studies and add weight to the modelling results.

8. RECOMMENDATIONS FOR FURTHER RESEARCH

These results have not only given insights into the likely flux of acidity from the sediments into the lakes but they also suggest further research that should be undertaken given the limitations of these results:

1. Monitoring of selected sites especially in the clayey soils should continue. This monitoring should include core sampling to determine the rate of sulfate reduction occurring.
2. Monitoring sites within lake sediments that were not exposed to oxidation during the recent drought should be considered to act as a control to the present sites.
3. Large columns could be obtained from the lake sediments and experiments on acid release from and sulfate reduction in these should be undertaken.
4. Modelling of the acid transport from these columns by coupling PHREEQC with HYDRUS2D/3D should be undertaken.
5. This modelling should be extended to consider the long-term future for the lakes. The present climate uncertainty is not likely to decrease, so the scenarios should include considering whether future acidification will be enhanced by the present conditions of the sediments and how this changes with the length of time the sediments are inundated.

9. REFERENCES

Adams, J.E. and Hanks, R.J. (1964). Evaporation from soil shrinkage cracks. Soil Sc i. Soc. Am. Procs., **28**: 281-284.

Addiscott, T.M., Thomas, V.H. and Janjua, M.A. (1983). Measurement and simulation of anion diffusion in natural soil aggregates and clods. Journal of Soil Science, **34**: 709-721.

Armstrong, J. and Armstrong, W. (1988). *Phragmites australis* – A preliminary study of soil-oxidising sites and internal gas transport pathways. New Phytologist **108(4)**: 373-382.

Bowman, G.M. and Hutka, J. (2002). Particle size analysis. In *Soil Physical Measurement and Interpretation for Land Evaluation*, Eds. McKenzie, N.J., Coughlan, K.J. and Cresswell, H.P., CSIRO Publishing, 224-239.

Bush, R.T., Fyfe, D. and Sullivan, L.A. (2004). Occurrence and abundance of monosulfide black oozes in coastal acid sulfate soil landscapes. Soil Research, **42**: 609-616.

Brooks R.H and Corey, A.T. (1964). Hydraulic properties of porous media. Hydrology Paper 3, Civil Engineering Department, Colorado State University, Fort Collins, Colorado.

Bush, R.T., Fyfe, D. and Sullivan, L.A. (2004). Occurrence and abundance of monosulfidic black ooze in coastal acid sulfate landscapes. Australian Journal of Soil Research **42**: 609-616.

Cook, F.J., Dobos, S.K., Carlin G.D.and G.E. Miller (2004). Oxidation rate of pyrite in acid sulfate soils: *in situ* measurements and modelling. Australian Journal of Soil Research **42**: 499-507.

Cook, F.J. and Knight, J.H. (2003). Oxygen transport to plant roots: Modeling for physical understanding of soil aeration. Soil Science Society of America Journal **67**: 20-31.

Cook F.J. and Cresswell H.P. (2008). Chapter 84 Estimation of Soil Hydraulic Properties. In *Soil Sampling and Methods of Analysis*. Eds Carter M.R. and Gregorich, Canadian Society of Soil Science, Taylor and Francis, LLC, Boca Raton, Fl, 1139-1161.

Cook ,F.J. (2011). Lake Alexandrina and Lake Albert: analysis of groundwater Measurements and Estimation of Acid Fluxes. Water for a Healthy Country National Research Flagship In Press.

Cresswell, H.P. (2002). The soil water characteristic. In *Soil Physical Measurement and Interpretation for Land Evaluation*, Eds. McKenzie, N.J., Coughlan, K.J. and Cresswell, H.P., CSIRO Publishing, 224-239.

Earth Systems (2008). Feasibility of Management Options for Acid Sulfate Soils in the Lower Murray Lakes. Stage 1: Preliminary Assessment of Treatment Options (Rev1). Consultants report prepared for Rural Solutions SA and the Department for Environment and Heritage, South Australia. December 2008.

Earth Systems (2010), Quantification of acidity flux rates to the Lower Murray Lakes. Prepared by Earth Systems Pty Ltd. for the Department for SA Department of Environment and Natural Resources, Adelaide.

Eching S.O., Hopmans, J.W. and Wendroth, O. (1994). Unsaturated hydraulic conductivity from transient multistep outflow and soil water pressure data. Soil Science Society of America **58**: 687-695.

EPA (2011). Lower Lakes Groundwater Acidification Risk Project Monitoring Report 2010. Environment Protection Authority South Australia.

DENR 2010, Acid sulfate soils research program summary report. Prepared by the Lower Lakes Acid Sulfate Soils Research Committee for the SA Department of Environment and Natural Resources, Adelaide.

Fitzpatrick, R.W., Marvanek, S.P., Shand, P., Merry, R.H., Thomas, M. and Raven, M.D. (2008). Acid sulfate soil maps of the River Murray below Blanchetown (Lock 1) and Lakes Alexandrina and Albert when water levels were at pre- drought and current drought condition, CSIRO Land and Water Science Report 12/08. CSIRO, Adelaide, 10 pages.

Fitzpatrick, R.W., Grealish, G., Chappell, A., Marvanek, S. and Shand, P. (2010). Spatial variability of subaqueous and terrestrial acid sulfate soils and their properties, for the Lower Lakes South Australia. Prepared by the Commonwealth Scientific and Industrial Research Organisation (CSIRO) Land and Water for the SA Department of Environment and Natural Resources, Adelaide.

Grossman, R.B., Brasher, R.R., Franzmeier, D.P. and Walker, J.L. (1968). Linear extensibility as calculated from natural-clod bulk density measurements. Soil Sci. Soc. Am. Proc., **32**: 570-573.

Hicks, W.S., Creeper, N., Hutson, J., Fitzpatrick, R.W., Grocke, S. and Shand, P. (2009). The potential for contaminant mobilisation following acid sulfate soil rewetting: field experiment, Prepared by The Commonwealth Scientific and Industrial Research Organisation (CSIRO) Land and Water, for the SA Department of Environment and Natural Resources.

Hipsey, M.R. and Salmon, S.U. (2008). Numerical assessment of acid-sulfate soil impact on the River Murray Lower Lakes during water level decline, Final Report, Centre for Water Research, The University of Western Australia.

Hipsey M.R., Bursch B.D., Colleti, J. and Salmon, S.U. (2010). Lower lakes Hydro-geochemical model development and assessment of acidification risks. Prepared by University of Western Australia for SA Water.

Kirby, J.M., Pierret, A., Moran, C.J., Cresswell, H.P., Cook, F.J., Knight, J.H. and Pankhurst C. (1998). GRDC Project CSO180, subprogram 3.5, *Final report: Hydraulic properties of subsoils: fundamental properties, and the role of biopores*. Report to Grains Research and Development Corporation. CSIRO Land and Water Consultancy Report, 98-58.

Lockington, D. A. (1994). Falling rate evaporation and desorption estimates. Water Resources Res., **30**: 1071-1074.

McGarry, D.J. (2002). Soil shrinkage. In *Soil Physical Measurement and Interpretation for Land Evaluation*, Eds. McKenzie, N.J., Coughlan, K.J. and Cresswell, H.P., CSIRO Publishing, 240-260.

McKenzie, N.J. andCresswell, H.P. (2002). Field sampling. In *Soil Physical Measurement and Interpretation for Land Evaluation*, Eds. McKenzie, N.J., Coughlan, K.J. and Cresswell, H.P., CSIRO Publishing, 11-34.

Philip, J.R. (1969). Theory of infiltration. *Adv. Hydrosci.* **5**: 215-96.

Philip, J.R. (1973). On solving the unsaturated flow equation: 1. The flux-concentration relation. Soil Science **116**: 328-35.

Rigby, P.A., Dobos, S.K., Cook, F.J. and Goonetilleke, A. (2006). Role of organic matter in framboidal pyrite oxidation. Science of the Total Environment **367**: 847-854.

Saxton, K.E., Rawls, W.J., Romberger, J.S. and Papendick, R.I. (1986). Estimating generalized soil-water characteristics from texture. Soil Sci. Soc. Am. J., **50**: 1031-1036.

Scotter, D.R., Clothier, B.E and Harper, E.R. (1978). Measuring saturated hydraulic conductivity and sorptivity using twin rings. Aust. J. Soil Res., **20**: 295-304.

Simpson, S., Jung, R., Jarolimek, C. and Hamilton, I. (2009), The potential for contaminant mobilisation following acid sulfate soil rewetting: lab experiment. Prepared by the Commonwealth Scientific and Industrial Research Organisation (CSIRO) Land and Water for the SA Department of Environment and Natural Resources, Adelaide.

Simpson, S.L., Fitzpatrick, R.W., Shand, P., Angel, B.M., Spadaro, D.A. and Mosley, L. (2010). Climate-driven mobilisation of acid and metals from acid sulfate soils. Marine and Freshwater Research, **61**: 129–138.

Šimůnek, J., and Šejna, M. (2007). The HYDRUS-2D Software Package for Simulating Two- and Three- Dimensional Movement of Water, Heat, and Multiple Solutes in Variably Saturated Media, User Manual, Version 1.02. PC-Progress, Prague, Czech Republic. 203p.

Sullivan, L.A., Bush, R.T., Ward, N.J., Fyfe, D.M., Johnston, M., Burton, E.D., Cheeseman, P., Bush, M., Maher, C., Cheetham, M., Watling, K.M., Wong, V.N.L., Maher R. and Weber, E. (2010). Lower Lakes laboratory study of contaminant mobilisation under seawater and freshwater inundation. Prepared by Southern Cross GeoScience for the SA Department of Environment and Natural Resources, Adelaide.

Tong, J. X., J. Z. Yang, B., Hu, X and Bao, R.C. (2010) Experimental study and mathematical modeling of soluble chemical transfer from unsaturated-saturated soil to surface runoff. Hydrological Processes, **24**(21): 3065-3073

van Genucten, M.Th., Leij, F.J. and Yates, S.R. (1991). The RETC code for quantifying the hydraulic functions of unsaturated soils. U.S. Salinity Laboratory, USDA ARS, Riverside, California, 85p.

van Genuchten, M. Th. 1980. A closed-form equation for predicting the hydraulic conductivity ofunsaturated soils. Soil Sci Soc. Am J. **44**: 892-898.

Warrick, A.W. (2003). Soil Water Dynamics. Oxford University Press Inc., New York, 391p.

Webster, I.T., Cook, F.J. and Hicks, W.S. (2008). Appendix C. Review of Hipsey and Salmon: Numerical Assessment of Acid-Sulfate Soil Impact on the River Murray Lower Lakes During Water Level Decline. In Peer Review of Acidification Thresholds for Lake Alexandrina and Lake Albert, Aquaterra (2008), 38-50.

White, I. and M. J. Sully (1987). Macroscopic and microscopic capillary length and time scales from field infiltration. Water Resources Research **23**(8): 1514-1522.

10. APPENDIX 1

Table 13. Moisture characteristic and bulk density (ρ_b) for Boggy Creek Site.

Site and Sample ID	Depth	θ at ψ = -0.1m	θ at ψ = -0.5m	θ at ψ = -1m	θ at ψ = -3m	θ at ψ = -6m	θ at ψ = -51m	θ at ψ = -154m	ρ_b (kg m^{-3})
BC1	0.03-0.05	0.54	0.53	0.51	0.47	0.44	0.29	0.26	1.21
BC1	0.05-0.07	0.56	0.55	0.53	0.47	0.44	0.34	0.31	1.15
BC2	0.03-0.05	0.60	0.56	0.53	0.45	0.41	0.26	0.24	1.06
BC2	0.05-0.07	0.56	0.51	0.48	0.38	0.32	0.18	0.15	1.17
BC3	0.03-0.05	0.59	0.57	0.56	0.50	0.46	0.49	0.46	1.09
BC3	0.05-0.07	0.57	0.54	0.51	0.44	0.40	0.30	0.25	1.15
Mean		0.57	0.54	0.52	0.45	0.41	0.31	0.28	1.14
Standard deviation		0.02	0.02	0.02	0.04	0.05	0.1	0.1	0.06
BC1	0.18-0.20	0.48	0.43	0.40	0.28	0.22	0.10	0.07	1.38
BC1	0.20-0.22	0.45	0.44	0.41	0.26	0.21	0.10	0.08	1.45
BC2	0.18-0.20	0.52	0.48	0.45	0.30	0.25	0.14	0.11	1.28
BC2	0.20-0.22	0.51	0.46	0.43	0.27	0.22	0.13	0.11	1.31
BC3	0.18-0.20	0.51	0.48	0.45	0.32	0.26	0.21	0.14	1.30
BC3	0.20-0.22	0.57	0.53	0.50	0.41	0.36	0.27	0.26	1.13
Mean		0.51	0.47	0.44	0.30	0.25	0.16	0.13	1.31
Standard deviation		0.04	0.04	0.03	0.06	0.06	0.07	0.07	0.1
BC1	0.38-0.40	0.48	0.45	0.42	0.24	0.20	0.13	0.09	1.37
BC1	0.40-0.42	0.48	0.45	0.42	0.23	0.19	0.10	0.09	1.37
BC2	0.38-0.40	0.51	0.48	0.44	0.25	0.21	0.11	0.08	1.29
BC2	0.40-0.42	0.48	0.45	0.41	0.21	0.17	0.09	0.06	1.38
BC3	0.38-0.40	0.50	0.46	0.42	0.26	0.21	0.13	0.10	1.32
BC3	0.40-0.42	0.52	0.48	0.45	0.29	0.23	0.17	0.08	1.27
Mean		0.50	0.46	0.43	0.25	0.20	0.12	0.08	1.33
Standard deviation		0.02	0.01	0.01	0.02	0.02	0.03	0.01	0.05

Table 14. Moisture characteristic and bulk density (ρ_b) for Point Sturt Site.

Site and Sample ID	Depth	θ at ψ = -0.1m	θ at ψ = -0.5m	θ at ψ = -1m	θ at ψ = -3m	θ at ψ = -6m	θ at ψ = -51m	θ at ψ = -154m	ρ_b (kg m^{-3})
PS1	0.03-0.05	0.57	0.32	0.25	0.15	0.08	0.06	0.01	1.15
PS1	0.05-0.07	0.54	0.29	0.22	0.19	0.11	0.07	0.04	1.22
PS2	0.03-0.05	0.47	0.26	0.18	0.12	0.07	0.03	0.02	1.42
PS2	0.05-0.07	0.43	0.26	0.15	0.09	0.07	0.04	0.03	1.52
PS3	0.03-0.05	0.47	0.24	0.16	0.11	0.06	0.01	0.01	1.40
PS3	0.05-0.07	0.50	0.26	0.16	0.12	0.07	0.01	0.01	1.33
Mean		0.49	0.27	0.19	0.13	0.08	0.04	0.02	1.34
Standard deviation		0.05	0.03	0.04	0.03	0.02	0.3	0.01	0.1
PS1	0.18-0.20	0.52	0.36	0.28	0.21	0.18	0.14	0.14	1.28
PS1	0.20-0.22	0.41	0.23	0.10	0.06	0.03	0.02	0.01	1.56
PS2	0.18-0.20	0.52	0.47	0.39	0.31	0.27	0.23	0.22	1.28
PS2	0.20-0.22	0.52	0.47	0.40	0.31	0.28	0.21	0.19	1.28
PS3	0.18-0.20	0.46	0.24	0.15	0.09	0.04	0.03	0.01	1.44
PS3	0.20-0.22	0.42	0.32	0.16	0.08	0.06	0.02	0.02	1.54
Mean		0.47	0.35	0.25	0.18	0.15	0.11	0.10	1.40
Standard deviation		0.05	0.1	0.1	0.1	0.1	0.1	0.1	0.1
PS1	0.38-0.40	0.38	0.31	0.24	0.16	0.13	0.07	0.07	1.64
PS1	0.40-0.42	0.39	0.35	0.30	0.20	0.17	0.08	0.10	1.62
PS2	0.38-0.40	0.36	0.32	0.27	0.15	0.13	0.06	0.05	1.70
PS2	0.40-0.42	0.39	0.31	0.21	0.11	0.09	0.06	0.03	1.63
PS3	0.38-0.40	0.36	0.32	0.24	0.15	0.11	0.06	0.05	1.69
PS3	0.40-0.42	0.36	0.30	0.19	0.10	0.08	0.02	0.02	1.69
Mean		0.37	0.32	0.24	0.15	0.12	0.06	0.05	1.66
Standard deviation		0.01	0.02	0.04	0.04	0.03	0.02	0.03	0.03

Table 15. Moisture characteristic and bulk density (ρ_b) for Campbell Park Site.

Site and Sample ID	Depth	θ at ψ = -0.1m	θ at ψ = -0.5m	θ at ψ = -1m	θ at ψ = -3m	θ at ψ = -6m	θ at ψ = -51m	θ at ψ = -154m	ρ_b (kg m^{-3})
CP2	0.03-0.05	0.82	0.77	0.73	0.66	0.62	0.55	0.51	0.49
CP2	0.05-0.07	0.82	0.79	0.76	0.68	0.65	0.60	0.55	0.48
CP3	0.03-0.05	0.82	0.77	0.73	0.63	0.60	0.53	0.49	0.48
CP3	0.05-0.07	0.81	0.75	0.71	0.60	0.56	0.40	0.39	0.51
CP4	0.03-0.05	0.81	0.80	0.77	0.70	0.67	0.52	0.48	0.49
CP4	0.05-0.07	0.83	0.80	0.78	0.70	0.66	0.52	0.50	0.46
Mean		0.82	0.78	0.74	0.66	0.63	0.52	0.49	0.48
Standard deviation		0.01	0.02	0.03	0.04	0.04	0.07	0.05	0.02
CP2	0.18-0.20	0.51	0.40	0.32	0.21	0.16	0.08	0.06	1.31
CP2	0.20-0.22	0.50	0.37	0.29	0.20	0.14	0.06	0.05	1.31
CP3	0.18-0.20	0.46	0.41	0.32	0.22	0.18	0.11	0.08	1.43
CP3	0.20-0.22	0.43	0.39	0.29	0.18	0.15	0.07	0.05	1.52
CP4	0.18-0.20	0.49	0.43	0.36	0.27	0.23	0.14	0.12	1.36
CP4	0.20-0.22	0.43	0.32	0.22	0.14	0.10	0.05	0.03	1.50
Mean		0.47	0.39	0.30	0.20	0.16	0.09	0.07	1.41
Standard deviation		0.03	0.04	0.05	0.04	0.04	0.03	0.03	0.09
CP2	0.38-0.40	0.50	0.47	0.40	0.28	0.24	0.15	0.14	1.32
CP2	0.40-0.42	0.56	0.51	0.45	0.34	0.29	0.24	0.18	1.17
CP3	0.38-0.40	0.66	0.62	0.55	0.43	0.40	0.33	0.31	0.90
CP3	0.40-0.42	0.67	0.61	0.56	0.43	0.39	0.31	0.30	0.87
CP4	0.38-0.40	0.64	0.63	0.59	0.48	0.43	0.34	0.31	0.94
CP4	0.40-0.42	0.71	0.67	0.63	0.52	0.47	0.37	0.34	0.78
Mean		0.62	0.58	0.53	0.41	0.37	0.29	0.26	1.00
Standard deviation		0.08	0.08	0.09	0.09	0.09	0.08	0.08	0.2

Table 16. Moisture characteristic and bulk density (ρ_b) for Boggy Lake Site.

Site and Sample ID	Depth	θ at ψ = -0.1m	θ at ψ = -0.5m	θ at ψ = -1m	θ at ψ = -3m	θ at ψ = -6m	θ at ψ = -51m	θ at ψ = -154m	ρ_b (kg m^{-3})
BL1	0.03-0.07	0.67	0.63	0.61	0.55	0.51	0.48	0.49	0.97
BL2	0.03-0.05	0.66	0.65	0.63	0.59	0.57	0.44	0.39	0.93
BL2	0.05-0.07	0.65	0.64	0.62	0.59	0.56	0.51	0.50	0.95
BL3	0.03-0.05	0.60	0.57	0.54	0.47	0.44	0.31	0.25	1.14
BL3	0.05-0.07	0.61	0.59	0.57	0.47	0.44	0.33	0.30	1.09
BL4	0.03-0.05	0.64	0.62	0.61	0.55	0.53	0.50	0.44	1.00
BL4	0.05-0.07	0.65	0.64	0.62	0.56	0.53	0.42	0.39	0.97
Mean		0.64	0.62	0.60	0.54	0.51	0.43	0.39	1.01
Standard deviation		0.03	0.03	0.03	0.05	0.05	0.08	0.09	0.08
BL1	0.18-0.22	0.61	0.57	0.54	0.47	0.42	0.32	0.23	1.14
BL2	0.18-0.20	0.65	0.63	0.60	0.54	0.51	0.35	0.33	0.99
BL2	0.20-0.22	0.66	0.64	0.60	0.54	0.51	0.39	0.28	0.96
BL3	0.18-0.20	0.53	0.50	0.46	0.35	0.32	0.17	0.13	1.34
BL3	0.20-0.22	0.51	0.48	0.44	0.34	0.29	0.14	0.10	1.38
BL4	0.18-0.20	0.45	0.43	0.37	0.25	0.20	0.11	0.19	1.51
BL4	0.20-0.22	0.51	0.49	0.46	0.38	0.32	0.22	0.15	1.36
Mean		0.56	0.53	0.49	0.41	0.37	0.25	0.20	1.24
Standard deviation		0.08	0.08	0.09	0.1	0.1	0.1	0.08	0.2
BL2	0.36-0.38	0.59	0.56	0.52	0.45	0.40	0.20	0.14	1.18
BL2	0.38-0.40	0.61	0.60	0.57	0.49	0.45	0.41	0.37	1.06
BL3	0.38-0.40	0.65	0.62	0.58	0.51	0.47	0.33	0.29	1.02
BL4	0.38-0.40	0.71	0.69	0.66	0.59	0.55	0.47	0.43	0.82
Mean		0.64	0.62	0.58	0.51	0.47	0.35	0.31	1.02
Standard deviation		0.05	0.06	0.06	0.06	0.06	0.1	0.1	0.1
BL2	0.36-0.38	0.65	0.64	0.61	0.53	0.49	0.44	0.40	0.96
BL2	0.38-0.40	0.69	0.66	0.63	0.55	0.52	0.33	0.31	0.90
BL3	0.38-0.40	0.65	0.62	0.59	0.51	0.48	0.39	0.36	1.00
BL4	0.38-0.40	0.75	0.72	0.69	0.63	0.59	0.44	0.41	0.73
Mean		0.68	0.66	0.63	0.56	0.52	0.40	0.37	0.90
Standard deviation		0.05	0.04	0.04	0.05	0.05	0.05	0.04	0.1